RWTH AACHEN UNIVERSITY

Opposable thumbs : A bare-hands text input technique

Master's Thesis at the
Media Computing Group
Prof. Dr. Jan Borchers
Computer Science Department
RWTH Aachen University

by
Hesham Omran

Thesis advisor:
Prof. Dr. Jan Borchers

Second examiner:
Prof.Dr. Torsten Kuhlen

Registration date: 06.03.2014
Submission date: 00.00.2014

I hereby declare that I have created this work completely on my own and used no other sources or tools than the ones listed, and that I have marked any citations accordingly.

Hiermit versichere ich, dass ich die vorliegende Arbeit selbständig verfasst und keine anderen als die angegebenen Quellen und Hilfsmittel benutzt sowie Zitate kenntlich gemacht habe.

Aachen, August 2014
Hesham Omran

Contents

List of Figures

List of Tables

Abstract

The finger tactile cues and anatomical configuration has intrigued many researchers for various functions and tasks. In a world where texting is an instant and intrusive communication through our daily life, we envision a system in which texting can be eyes free. As the first step, this paper investigates the precision of the thumb in pressing on targets on the finger skin while no visual feedback of the hand. Through an experimental study, our preliminary study showed that users precision is influenced by tactile cues on the skin of the fingers specially on the different phalanges of the finger. Furthermore, we were able to capture and report users hand postures, discomfort, localisation strategies of the targets and the effect of different fingers on targets accuracy. Using data mining and data partitioning techniques we were able to compute an effective imaginary keyboard layout, which can capture effectively users interaction, nevertheless, the limitation of this layout was also communicated for future work.

Acknowledgements

Foremost, I would like to express my special appreciation and thanks to my advisor Chatchavan Wacharamanotham. I would like to thank him for his patience and immense knowledge. His guidance helped me in all the time of research and writing of this thesis.

I would like to thank the Media Computing Group, for their tremendous support and feedback throughout the period of my thesis. I would also like to thank my thesis advisor, Prof. Dr. Jan Borchers, and Prof. Dr. Torsten Kuhlen, my second examiner.

Furthermore, I would like to thank all the participants, who voluntarily took part in my user studies, and sacrificed their time and effort. Finally, I would like to thank my family for supporting me mentally and morally through the course of this thesis.

Thank you!

Hesham Omran

Conventions

Throughout this thesis we use the following conventions.

Text conventions

Definitions of technical terms or short excursus are set off in coloured boxes.

EXCURSUS:
Excursus are detailed discussions of a particular point in a book, usually in an appendix, or digressions in a written text.

Definition: *Excursus*

Definitions of hypotheses are set of in yellow-colored boxes.

HYPOTHESIS:
A supposition or proposed explanation made on the basis of limited evidence as a starting point for further investigation.

Description: *Hypothesis*

The whole thesis is written in Canadian English.

Chapter 1

Introduction

Today, as more portable computers and wearable on-body devices emerges such as smart glasses and smart watches, one of the limitations of these devices is the lack of text input. Other alternatives such as microphones with voice recognition can also be inconvenient due to the ambient noise from the surrounding environment or in case of needing to text sensitive or confidential data.

Recent wearables lack discretion in text input methods.

Wearable on-body interfaces (Harrison et al. [2012]) such as the text input gloves KITTY (Mehring et al. [2004]) and Gauntlet (Liu [2012]), tackled the aforementioned problems. On the other hand, these types of wearables tend to be intrusive during users interaction with the physical environment. As the glove needs to be wore during interaction, and demands more attention from the user to target the appropriate keys on the glove for texting.

Gustafson et al. [2010] introduced the concept of imaginary interfaces, as they proved through a series of studies, that users can interact with invisible interfaces with no visual content projected. Using spatial landmarks e.g. on the hand such as shape of the palm or skin folds, a cognitive mapping can be established between the virtual interfaces and the visual and tactile cues, such as the touch and sight of the palm of the hand.

Imaginary interfaces are invisible UIs, which the user can link it's virtual functionality to a physical device.

Gustafson et al. [2013] demonstrated that even in the absence of the visual sense of the user e.g. users blinded from seeing the palm of their hands. The tactile sense which comes from the sense of touch, and proprioceptive ability when using an on-body interface, can still allow a successful interaction with the invisible UIs.

Existing new sensor technologies and wearable devices allow capturing finger interaction with no need for gloves.

Furthermore, there exists different implementations which allows on-body thumb and finger interaction with no need for the use of gloves. PinchWatch (Loclair et al. [2010]), a vision based system which tracks the thumb movement over the palm. Using a depth camera mounted on the chest, gestures of the thumb over the fingers and palm can be captured.

Additionally, more devices are emerging which utilises non vision based sensor, such as electromyography sensor and accelerometers. FIN (RHLVisionTechnologies [2014]) is a wearable ring that you can wear on the thumb of your hand, while It tracks the movement of thumb and converts it to different gestures. While, MYO (ThalmicLabs [2013]) developed by thalamic labs is an armband that can detect subtle electrical pulses generated by the muscle during movement and map gestures to these movements.

These devices can prove to be an alternative for gloves, while keeping the tactile sense for blinded interaction with imaginary interfaces.

1.1 Motivation

We observed the absence of a user oriented study concerning the thumb on finger interaction, which focuses on the different human hand characteristics.

We focus on 3 characteristics of the hand, it's anatomy, proprioceptive ability, and tactile landmarks.

Discussed further in chapter 3, in our study we focus on 3 characteristics of the hand. (1) Fingers and thumb anatomy e.g. the articulation of the hands and joints, and finger cylindrical shape, (2)proprioceptive ability in an eye's-free interaction e.g. it's ability to locate itself even in absence of the visual sense, and finally, (3) the tactile landmarks on the finger's skin e.g. creases on the fingers.

We aimed to measure (1) how precisely and effectively users can touch certain areas on their finger, given being near to or located on certain landmarks, and on the sides of the finger ?, in absence of their visual sense, and only focusing on tactile and proprioceptive sense. (2) How will the users use these tactile landmarks during selection ? and (3)how and which areas in which users felt physical strain of their hands, specially with repetitive selection ?.

1.2 Contribution

This thesis contributes with measuring the proprioceptive ability and tactile sense of the finger and thumb interaction, Designing and evaluating layouts, and parameters needed for such layouts. Furthermore, using these outcomes as a design guideline for future implementations of the touch keyboard layout on the fingers and palm, such as a QWERTY Layout Keyboard.

Understanding the areas around and on the landmarks can help enhance the imaginary touch keyboard layout for texting.

Finally, contrasting the finds of these layouts such as the touch width, precision and effectiveness to other similar on-body interactions, which are mentioned in chapter 2 “Related Work”.

1.3 Overview

In chapter 2 “Related Work”, will be demonstrated similar work evaluating on-body interaction precision and effectiveness, and the concept of imaginary interfaces. These studies inspired our user study methodology and research question. Furthermore, other related work on the implementation of new hand gesture recognition technologies will be reviewed.

In chapter 3 “Design Approach”, we will demonstrate thoroughly the different aforementioned characteristics of the thumb and finger. Moreover, demonstrating the mathematical formulas and instruments used to realise and test our interaction.

In chapter 4 "User Study : The Conceptual Layout", we will demonstrate the developed hypotheses. Revealing our conceptual layout rationale developed based on the characteristics in chapter 3 "Design Approach". Furthermore, Revealing the study procedure and data correction methodology. we will analyse the conceptual layout both quantitatively and qualitatively.

In chapter 5 "Layout Evaluation", we will evaluation of the effectiveness of our conceptual layout through the use of distance-based classification and cross validation to overcome our limited data points. we will derive different layouts from our original layout to find a layout that reach effectiveness of above 90 % and attain the maximum number of touch points per finger. Finally, we will discussing the implication of these findings on the overall design of the thumb over finger interaction and limitation of the study.

In 6 "Summary and future work", the summary and future work.

Chapter 2

Related Work

In the previous chapter, we have established the need for a user oriented study to address the emerging technologies that utilise the thumb on finger interaction. Nevertheless, another issue needs to be tackled is the lack of visual feedback or visual display on the hand, eyes-free interaction and the utilisation of the different characteristics of the finger and thumb. Furthermore, demonstrating enabling technologies that can be prominent for such an interaction.

Previous work have established already different concepts which have affected our research path. In this chapter we will demonstrate these researches findings, and how it affected our work. publications have been categorised in the following sections :

2.1 Imaginary Interfaces : The Role of Visual and Tactile Sense

Imaginary interfaces, is a discipline that assumes interaction with screen-less devices that allow 2D spatial interaction with invisible interfaces without any visual feedback. Researches concerned with exploring how imaginary interfaces function. Moreover, how different landmarks, visual or touchable can allow or even enhance users experience,

imaginary interfaces, assumes users can interact with invisible interfaces without visual feedback.

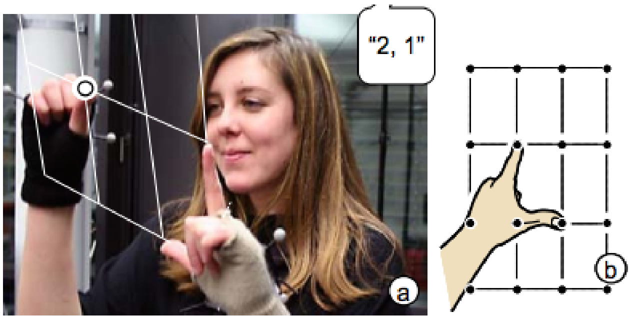

Figure 2.1: Imaginary Interfaces : (a) Participant selected a target at the coordinate announced by the system. (b) Partici- pants acquired 16 positions from (-1,-1) to (2,2).

and be used to guide them during their interaction with invisible UIs.

Gustafson et al. [2010], developed the concept of imaginary interfaces. One tasks in their user study involved pointing to imaginary targets by announcing certain location coordinates. participants raised their hands, forming an L shape gesture with their index finger and thumb, as shown in figure 2.1. Furthermore it was shown that accuracy near the landmark increased, while it decreased gradually, as participants point away from them.

The visual sense and tactile surface verses non visual tactile-less surface.

Gustafson et al. [2011], used the same empty hand technique to investigate transfer learning in which participants were asked to recall and select apps on their iPhone home screen from memory, in the absence of any visual display on the hand e.g. pico-projector in sixth sense (Mistry and Maes [2009]). Participants used the L shape empty hand technique and the palm of their hands as an alternative to their iPhone. Comparing the visual sense and tactile surface against non visual tactile-less surface.

The palm richness in landmarks and tactile feedback allowed more accurate results over the empty space.

They discovered that due to the palm richness in landmarks and tactile feedback, it allowed more accurate in recalling and selection over using the empty hand. Also, the palm landmarks allowed symbolic association to the interface e.g. buttons or icons. In their investigation they used the crease of the hand and palm to create a grid like inter-

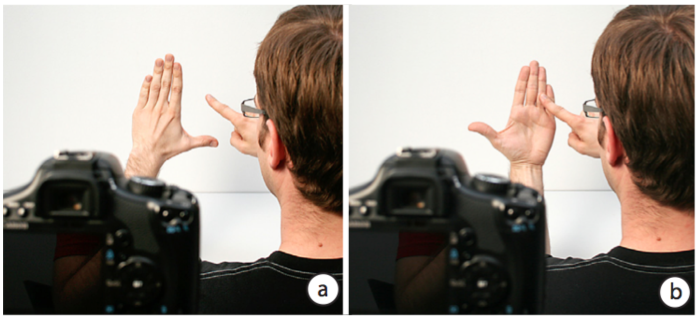

Figure 2.2: Imaginary Interfaces : Study 2 apparatus: (a) empty space condition and (b) palm condition.

face similar to the home screen of the iPhone. When comparing the performance of touching on the palm against the empty hand, it was shown that the average standard deviation of touches, and the computed circular minimum button diameter on the empty space interface was 27.9mm (SD = 0.32) in comparison to 17.7mm (SD = 0.22) on the palm interface. It was reported by Gustafson's that these results difference were statistically significant (t11=2.912, p=0.014, Cohen's d=0.84). The distribution of the touch points on the palm and empty hand is demonstrated in figure 2.3

Interaction on the palm resulted in a button size of 17.7mm in diameter compared to empty hand with 27.9mm diameter.

Finally, Gustafson et al. [2013] investigated further in the visual sense which allowed subjects to control imaginary interfaces from watching their hands during interaction. In one of their studies, they tested the tactile cues and the human proprioception of the palm-finger interaction when removing the visual sense by blindfolding participants.

Furthermore, similar to the experiment conducted in Gustafson et al. [2011], in which users asked to recalled apps from the memory and visualise their iPhone home screen in their head, using the palm and finger instead of their iPhone. as shown in figure 2.4, the subject's finger was covered to remove tactile sensation from the finger on the palm. Moreover, subjects were asked perform the same task on a fake silicone palm, instead of their real palm to remove the tactile sensation from the palm, while keeping the tactile feeling on the finger. They conducted the experiment for both conditions, participants were sighted and blind-

Users need the sensation on their palm, more than the need of sensation on the tip of their selecting finger.

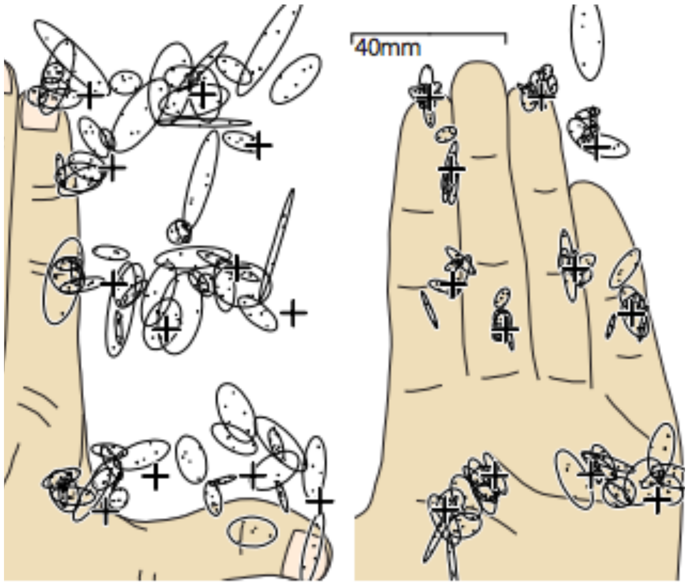

Figure 2.3: Imaginary Interfaces : All touches from all participants for (left) the empty space condition and (right) the palm condition. Plus signs indicate actual target positions. Ovals represent the bivariate normal distribution of selections per participant per target.

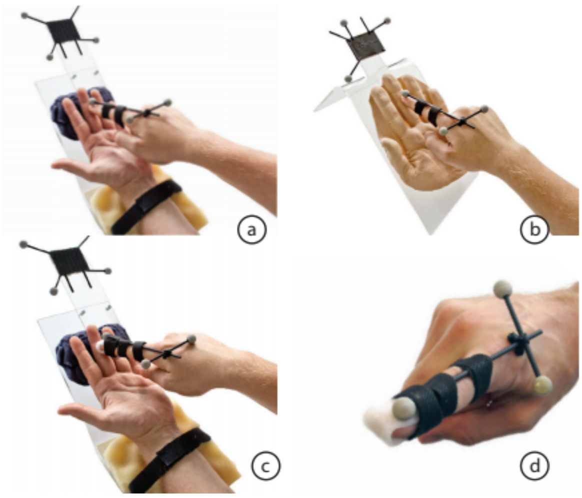

Figure 2.4: Imaginary Interfaces : Study 3 conditions (a) PALM vs. (b) FAKE PALM vs. (c) PALM WITH FINGER COVER; (d) close up of finger cover.

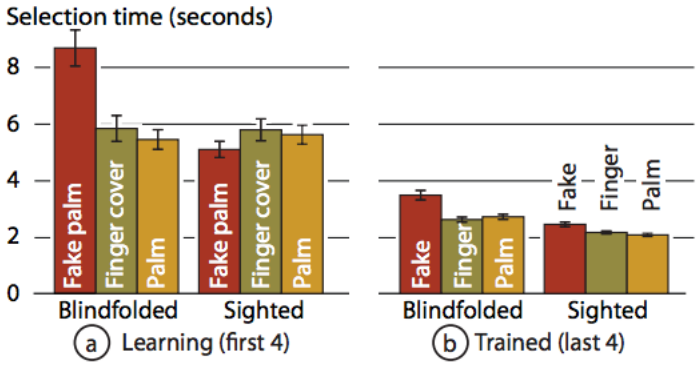

Figure 2.5: Imaginary Interfaces : Study 3 results showing the (a) first and (b) last half of the repetitions. Error bars are +/- one std. error.

folded.

As demonstrated in figure 2.5, the fake palm had the worst performance when participants were blindfolded, while the normal palm interaction and the covered finger both performed similarly.

it was derived from their study that :

1. In absence of visual cues, tactile cues available for the pointing finger filled in for the visual cue making the palm based imaginary interface usable even when operated eyes-free.

2. While it was expected the most of the sensing of the tactile cues is on the pointing finger, the study showed that the passive tactile sense of the palm is more important, as it allow users to orient themselves. Therefore, it was deducted that tactile cues sensed by the palm are unique and allow users to easy locate spatially, than the tactile cues sensed by the fingertip.

Usiing the landmarks on the finger can elevate the eyes-free imaginary keyboard interaction.

Gustafson's work on imaginary interfaces lead us to research in the absence of the visual sense, and dive into the eye's-free interaction. His findings concerning the landmarks on the palm of the hand and tactile sense directed us towards investigating more about the landmarks on the finger and how precious can this touch based imaginary layout achieve in an eyes-free interaction. Furthermore, We ought to measure the time needed to select and confirm selection of a certain areas around different landmarks and how physically is it convenient for the users with repetitive work such as texting. Finally, to investigate which landmarks on the hand are easier to relate to and locate on the hand, compared to other landmarks using the tactile and proprioceptive sense only.

This investigation lead us to the next section in which we review similar on-body eyes free interaction, where we laid out their findings and how they performed their user studies.

2.2 Evaluating Eyes-Free Interaction & On-Body Landmark Effectiveness

On-Body interactions using the tactile and proprioceptive sense can be superior to any external devices in eye-free interaction.

As the sensing technologies advances, on-body interactions allowed new possible interfaces using the body as an input and output platform. Across our literature review, it was found that on-body interaction granted users the proprioceptive ability of the body, which allows the ability to locate ones own body parts without the need for visual feedback e.g. sight of ones hand. Combined with the tactile sense, eyes-free interaction can be superior incase of the lack of a visual display, to any other external device such as e.g. phone, remote.

In this section we will review publications which aimed to measure the effectiveness of the proprioceptive ability of the body and the effects of tactile cues on the interaction experience.

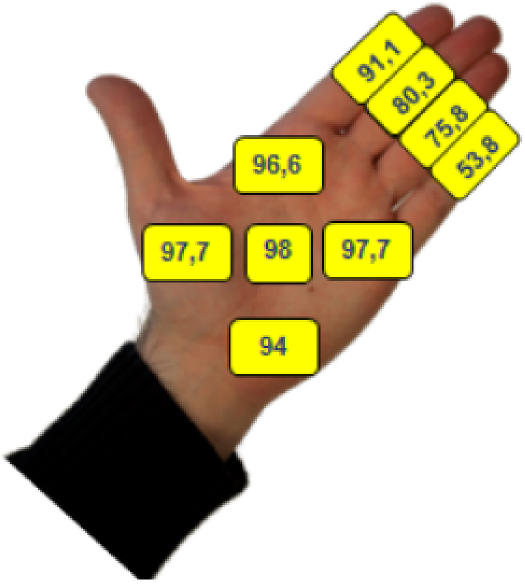

Figure 2.6: PalmRC : Average effectiveness percentage of targeting each landmark without visual demand.

Dezfuli et al. [2012] investigated the use of palm imaginary interfaces and eyes free interaction. They ought to investigate a conceptual design for an on-body remote control. Aiming to measure it's effectiveness and gain feedback on the interaction. In their investigation, the authors used the palm landmark as a leverage to their eyes free interaction. Participants were asked to interact with the content projected on the TV without looking to their hands.

Using imaginary interfaces to design an on-body remote control which allows an eyes free interactions with the TV.

Dezfuli used the 4 convex and 1 concave regions of the palm and the fingers as shown in figure 2.6, using the mentioned features of the palm as landmarks to map the remote control functions. The results of his research showed that on average, the diameter necessary to encompass 90% of all touches was 28mm (SD= 0.85). All of the palm landmarks were effectively touched with at least 94% effectiveness. The finger landmarks were less effectively touched with as little as 53% for the pinky.

Finding tactile landmarks on the palm, which the users can find easily and touch effectivily.

Furthermore, another task was to determine the resolution of touching targets over the palm. The participants were

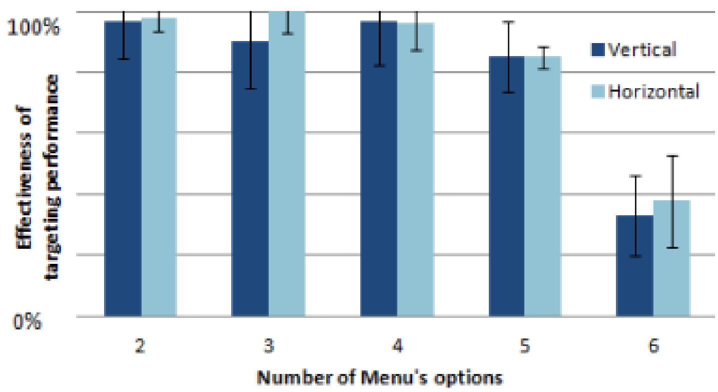

Figure 2.7: PalmRC : The average effectiveness of targeting vertical and horizontal grids with different equal-sized options.

the number of menu options that can be showed on the screen and the user can emulate preciously on her palms not more than 5 targets next to or under each other

asked map the UI shown on the projected screen in front of them, to touching on the palm of their hands. Participants were asked to touch a number of consecutive targets on the palm of their hands in both vertical and horizontal direction of the targets on the palm. Targets started from 2 up to 20 targets consecutively under or next to each other, depending on the orientation. Thereafter the success rate for targeting was calculated. As shown in figure 2.7, the effectiveness is above 90% until the 5 targets layout, and decrease severely hereafter.

On the other hand, Earput (Lissermann et al. [2013]), also aiming to measure the proprioceptive ability of the body. They investigated the affordance of the human ear for an on-body mobile interaction, their study showed that there are salient regions on the ear in which participants were able to touch effectively and preciously.

Earput tries to find the precision and effectiveness of the proprioception and tactile features of the ears.

In their experiment, Lissermann et al. [2013] ought to understand how reliable will the sense of proprioception allows the touch of targets over ones own ear. They ought to answer these 2 questions (1) how precisely and effectively users can touch certain areas ?, and (2) how many different areas can be targeted on the ear ?. The task involved map-

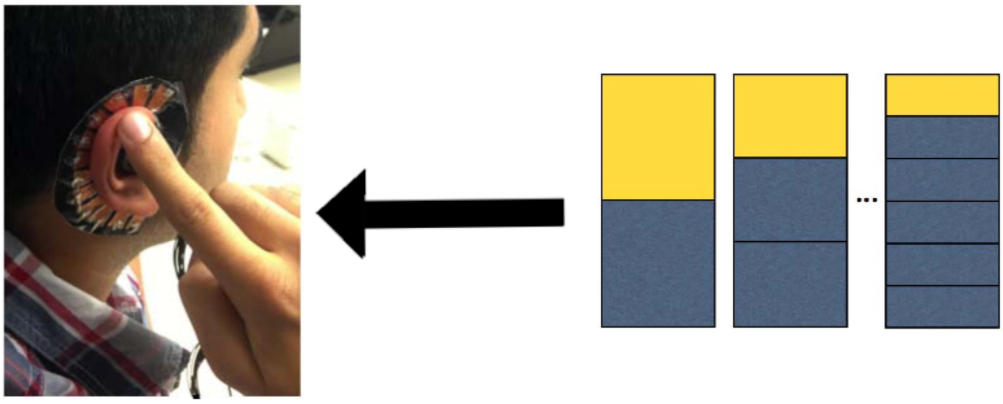

Figure 2.8: EarPut : Region based user interfaces used in the experiment. The UIs were subdivided into 2 to 6 areas, requiring the participants to touch the highlighted areas.

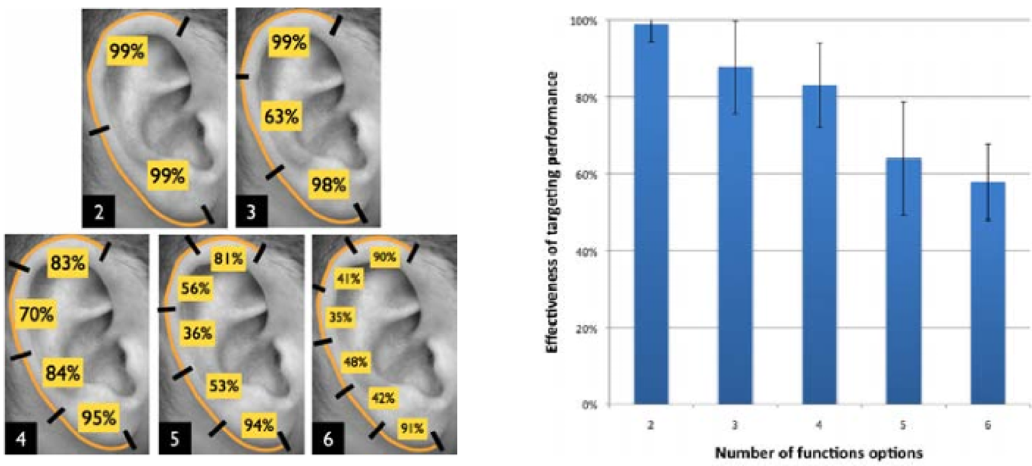

Figure 2.9: EarPut : The average effectiveness of targeting areas per region-based user interface.

ping a visualised 1D region-based interface to the arc of the ear and touch the highlighted area, as shown in figure 2.8.

Lissermann results as shown in figure 2.9, that as more regions added decreases the effectiveness of the touch. While overall on average the effectiveness is above 80%. the results and their semi-structured interview with the participants showed that it was hard to distinguish between more than 4 regions on the ears. Furthermore, parts of the ear that can be realised as landmarks such as the ear lobe and

Effectivness found overall above 80% and up to 4 regions of touch on the arc of the ear.

top arc of the ear had accuracy above 90%. While for the middle part of the ear was less distinctive, as it's effectiveness was below 80%.

Our aim is to build a conceptual model of the thumb on finger touch using the tactile and proprioceptive ability of thumb and fingers.

Following their same methodology, our aim is to measure the precision of the thumb over finger interaction, and how many areas can be targeted on phalanges of the fingers given certain landmark mentioned in details in chapter 3 "Design Approach" and 4 "User Study : The Conceptual Layout". Finally, measure the effectiveness of overlaying a series of keyboard buttons over the fingers, and comparing our finding concerning the proprioceptive ability of the subjects using thumb-finger interaction to the related work mentioned.

In the next section, we will mention different implementations, these implementations steered our direction towards the finger and thumb interaction, rather than a palm and index finger mentioned in the previous literature.

2.3 Implementations & Existing Technologies

Wearables could be smart glasses, smart watches or can be on clothes fixtures, such as small sensors.

Wearables are body-borne computers, which users wear under, on top of or within their clothing. Wearables can be general or special purposed machines developed for information technology and media development. such wearables could be smart glasses, smart watches or can be on clothes fixtures, such as small sensors.

In our literature review, we found numerous wearable systems, that either implemented a thumb on finger interaction such as PinchWatch, FIN and MYO. While other implementations tackled the texting implementation on the hand such as KITTY and Gauntlet, a glove based texting on the hand.

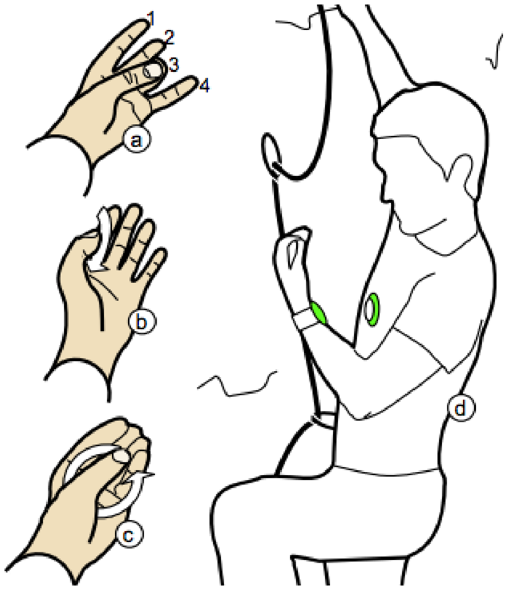

Figure 2.10: PinchWatch : The PinchWatch device supports (a) discrete input (pinching different fingers and finger segments), (b) sliding along the fingers and (c) dialling on the palm. All interactions involve users touching their palm or fingers with their thumb, which offers physical feedback and thus allows for eyes-free use. (d) Because the user's hands are empty, the user is, at anytime, able to immediately abandon interaction and use both hands in the physical world.

PinchWatch was designed to allowing the use of only one hand for operation, while other hand for the physical task in demand.

Loclair et al. [2010] presented a wrist-mounted display and chest-mounted camera, as shown in figure 2.10 which captures gestures and interaction made by the thumb on finger. Their aim was to design a wearable system which allows users to interact with the physical environment, and to be able to abandon interaction with the device instantly when the physical environment requires user's attention.

PinchWatch was designed to decrease interference with the user primary task. (1)By removing the need for modes and menus, thus focusing on gesture based interaction. (2)Utilising the hand tactile feedback and Proprioception to enable eyes-free use. (3)Finally, as one of the use cases of this system is for the user to be able to instantly interact with

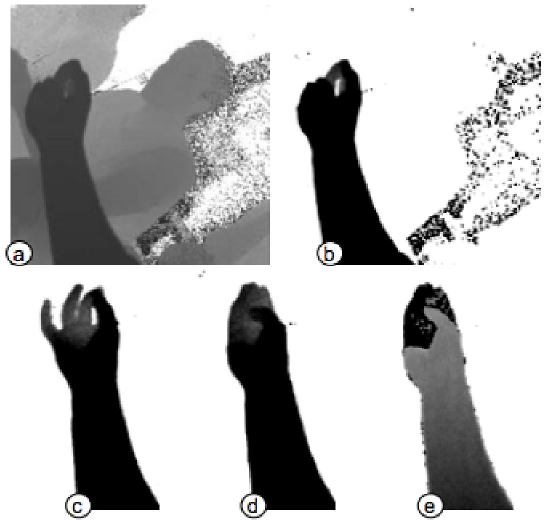

Figure 2.11: PinchWatch : Depth camera images: (a) raw image with depth encoded as grayscale; (b) threshold applied to separate hand from background; (c) pinch on middle finger; (d) thumb on hand; (e) thumb on hand with extra processing to increase local contrast.

the physical world when needed. They aim to design the interaction to only involve single hand use.

PMD cam cube 2.0 time-of-flight allowed robust separation of the fingers and thumb interaction, compared to standard RGB camera.

Loclair experimented with different vision based capturing systems to realise the design aforementioned. Mainly the standard RGB camera and the PMD Camcube 2.0 time-of-flight depth camera suggested by Kolb et al. [2009]. The depth camera allowed separation of the background from foreground, even in direct sunlight compared to the standard camera which needed a ring of IR LEDs to overcome lighting problems. Finally, the depth information can be used to separate parts of the hands, such as in figure 2.11. In which the thumb and and palm of the hand are separated by a depth threshold.

KITTY aimed to decrease the number of keys on the keyboard, increase portability and keep the traditional QWERTY layout.

KITTY (Mehring et al. [2004]) on the over hand, is a hand mounted glove which support touch typing. The authors aimed to decrease the keyboard size and increase portability while maintaining the traditional QWERTY layout. To overcome the limitation of some designs currently available such as the foldable keyboards, which reduces size of

Figure 2.12: KITTY : Prototype glove system illustrating initial contact placement.

the keyboard, but when needed it returns again to full size. Other designs decreased the number of keys rather than reduce the size of the key to achieve this size reduction, this can lead to added complexity to switch between certain states to add more alphanumerics per key. Furthermore, some wearable keyboards are very portable but could be restraining, such as Gesture pad by Sony.

KITTY aim to provide an intuitive access to the common touch typing skill, while following he traditional QWERTY layout. KITTY uses the combination of multiple contacts of the finger and thumb to activate the key press event. Nevertheless, a significant advantage is that KITTY allows you to use your hands without accidentally inputing data as long as finger and thumb of the same hands do not meet.

KITTY aimed to utilise the intuitiveness of touch typing over the traditional QWERTY keyboard, by allowing fingers to touch type on thumb.

The prototype is a wired electrical contact points placed on the tips of the fingers, thumb and palm of a wearable glove as shown in figure 2.12. Furthermore, the wiring of the contact points follow a similar patterns of 10 fingers touch typing over the keyboard. Using the thumb as the support base for clicking, as shown in figure 2.13.

Similar to the 10 finger touch typing in access the 1, Q, A and Y letters in rows 1, 2, 3 and 4 consecutively on the keyboard we use our pinky finger. Hence, on the glove to acti-

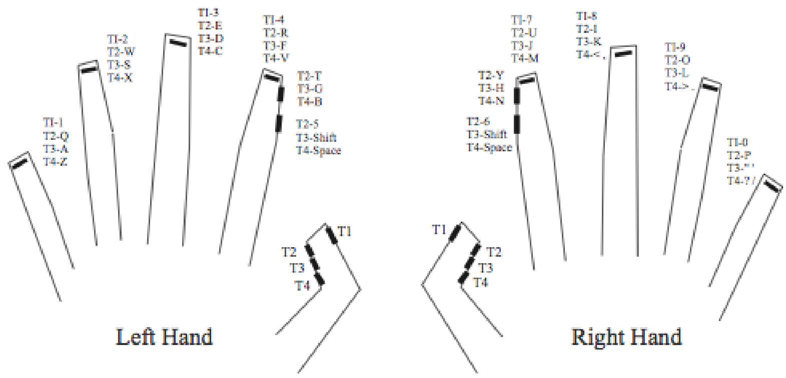

Figure 2.13: KITTY : Keyboard to glove mapping of wireless KITTY implementation.

vate either 1, Q, A or Y by pressing the pinky finger against the contact points T1, T2, T3 and T4 consecutively on the thumb. Similarly, the same methodology for all the other keys. The full keyboard layout map is shown in figure 2.13.

Physical discomfort at during at the pinky finger and thumb lower pad interaction. hand size variation introduced a limitation

In conclusion, the authors had some concerns and notes on the interaction design, such as for touching the pinky with T4 contact point lower pad of the thumb had an awkward feeling, with speculation of strain of this unaccustomed position. Furthermore, also the variation in lengths of the hand and fingers forced the authors to accommodate for changing contact points positions by using half ring mount clips.

Gauntlet over lay each two keyboard letters above each other in between each joint of the finger.

G.A.U.N.T.L.E.T (Liu [2012]) or Generally Accessible Universal Nomadic Tactile Low-power Electronic Typist is also another hand glove that is used for typing. GAUNTLET places keys in between joints of each finger, as shown in figure 2.14. Putting each two keys adjacent to each other along the width of the finger. Furthermore, Gauntlet also aimed for a one hand use keyboard to allow users to interact with other tasks with the other, similar to the concept of PinchWatch (Loclair et al. [2010]). There was no mention of the keyboard layout design or the methodology behind the placement of the keys except what was demonstrated in the figure aforementioned and video in their reference online page.

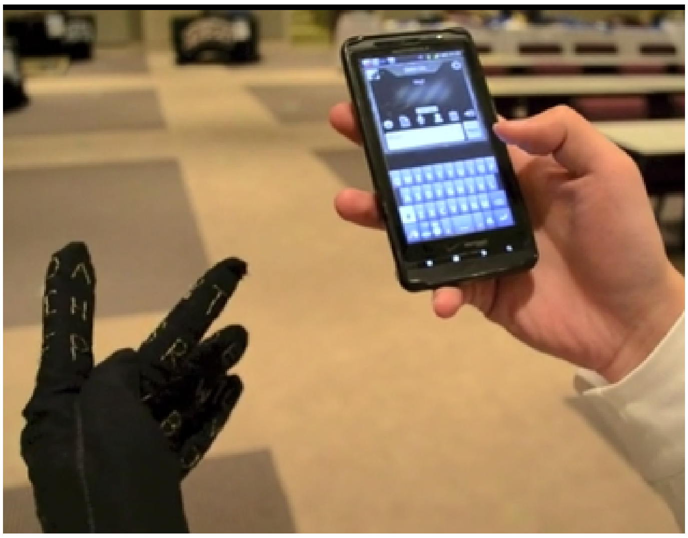

Figure 2.14: GAUNTLET : Keyboard glove implementation connected to a mobile phone via bluetooth.

Finally, we demonstrate some of the commercial off the self technologies, which are non vision based systems, and does not require to wear a glove or a heavily intrusive device to interact with. Therefore allow feeling of the hand and thumb tactile sense while interaction. These systems uses various sensors such as electromyography, accelerometers ... etc., to recognise and activate gestures for control and interaction.

New emerging wearable systems utilising accelerometers and electromyography sensors for hand interaction.

FIN (RHLVisionTechnologies [2014]) is tiny wearable device that you can wear on the thumb of your hand as a ring. It tracks the movement of thumb and converts it to different gestures, while It can also track each part of the finger.

MYO (ThalmicLabs [2013]) is also a wearable device developed by thalamic labs, which also detects the subtle motion of the arms and hands of the user through the use of EMG (electromyography) technology. The MYO armband lets you use the electrical activity in your muscles to wirelessly control your computer, phone, and other favourite digital technologies.

Finally, as most implementations of a text input over

Figure 2.15: Commercial Wearables : FIN (left) interface and interaction design, MYO (right) thumb on finger gesture .

The limits of the human proprioceptive and tactile sense need to be studied, to guide these new devices.

the hand devices such as GAUNTLET or KITTY, have used the thumb over hand interaction. While, other new emerging technologies such as FIN and MYO used this thumb over finger interaction. Moreover, other systems which aim for single hand use interaction such as PinchWatch. It lead us to investigate and build a touch button layout over the hand which test the use of a the thumb over finger interaction, similar to Earput and PalmRC.

Chapter 3

Design Approach

In this chapter, we will demonstrate the different characteristics and anatomy of the hand, such as the hand articulation and tactile features. Moreover, we will demonstrate our kinematic hand model and our tracked features for the finger and thumb touch interaction. Furthermore, we review our mathematical transformations,which we applied on these feature points to extract the touch events. Finally, we demonstrate the configuration, advantages and disadvantages of the instruments we used to extract our feature points.

3.1 Hand Anatomy & Characteristics

In this section, we will demonstrate the characteristic of the hand such as the articulation of the hand, the bone structure and the involved joints and it's degrees of freedom. Describing the sets of different movements performed by the thumb and fingers, and how they affected our choice of feature points to track. Moreover, we will demonstrate our classification of the tactile landmarks of the skin and finger shape. Finally, the proprioceptive ability of the hand.

Demonstrating finger and thumb articulation, finger tactile landmarks, and proprioceptive ability of the hand.

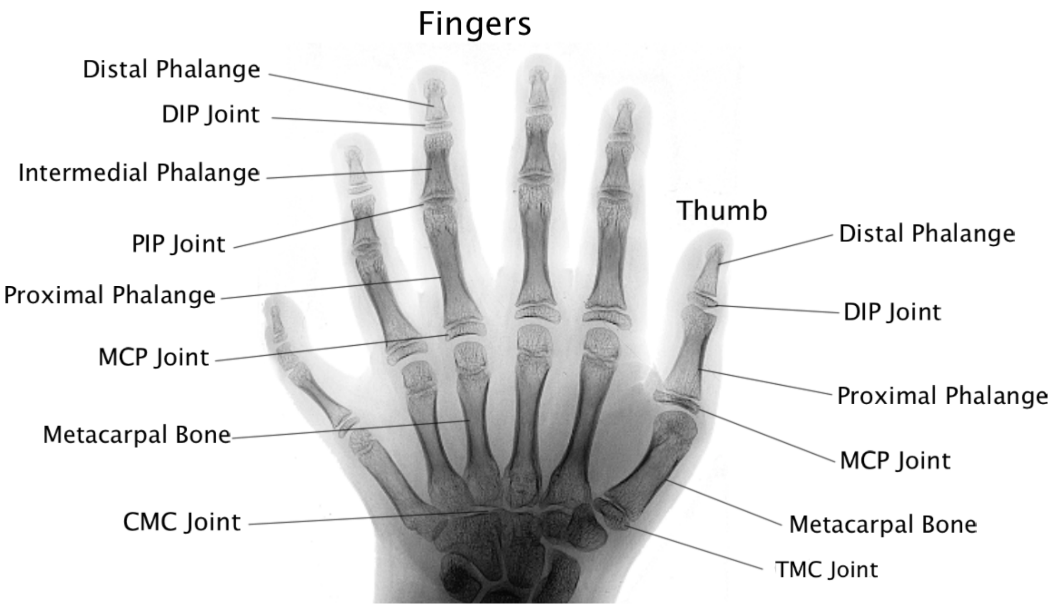

Figure 3.1: Hand Anatomy : Labeled skeleton of the bones and joints structure of the fingers and thumb of the hand.

3.1.1 Fingers & Thumb Articulation

Four Fingers

Each finger have 3 phalanges, the IP joints connects the phalanges. While the MCP joint connect the finger to the palm of the hand.

Each of the four fingers are composed of 3 phalanges , which are bones found in the fingers of most vertebrates. Starting from the fingertip, The distal phalange is followed by the Intermedial phalange, then, the proximal phalange. Finally, the metacarpal bone which lies in the palm of the hand, connecting the palm to the proximal phalange.

Furthermore, each of the phalanges are separated by an IP (Interphalangeal) joint, as shown in figure 3.1. The IP joints act as hinges between the phalanges of the hand, with 1 DoF (Degrees Of Freedom) allowing only one set of movement allowed by the IP joints, which is the flexor(A)/extensor(B) set (Rath [2011]), as demonstrated in figure 3.2.

IP joints allow a 1DoF motion of the phalanges

The IP joints of the finger are the DIP (Distal Interphalangeal) joint and the PIP (Proximal Interphalangeal) joint.

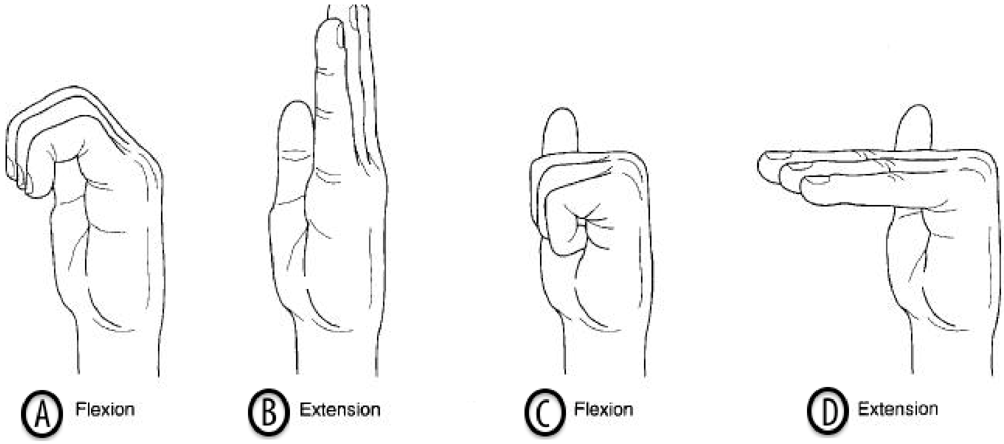

Figure 3.2: Finger Articulation : The types of movements of the MCP and IP joints of the fingers, (A) Flexion of the IP joints and extension of the MCP joints (B) Extension of IP joints and MCP joints (C) Flexion of the IP and MCP joints (D) Flexion of the MCP joint and Extension of the IP joints .

The DIP joint allows the articulation between the distal and Intermedial phalange, and the DIP joint allows the articulation between the Intermedial and proximal phalange.

The MCP (Metacarpophalangeal) joints connects the fingers to the hand palm. The MCP joint provides 2 degrees of freedom, thus allowing two sets of movements, The flexion(B)/extension(D) set as shown in figure 3.2, and the abduction(A)/adduction(B) set as shown in figure 3.3 (Rath [2011]). Moreover, The middle finger is the point of reference for the abduction and adduction, as the middle finger does not move during the adduction movement (Lippert [2011]).

The MCP joint allow a 2DoF motion of the whole finger. Flexion & extension, and abduction & adduction movement.

Finally, the CMC (carpometacarpal) Joint lies in the wrist which allows articulation between the wrist of the hand and the metacarpal bones. This structure allows the palm to arc when grasping objects.

The Opposable Thumb

The thumb is composed of 3 phalanges with similar anatomy to the finger, expect the absence of the

The thumb anatomy has different structure than the fingers.

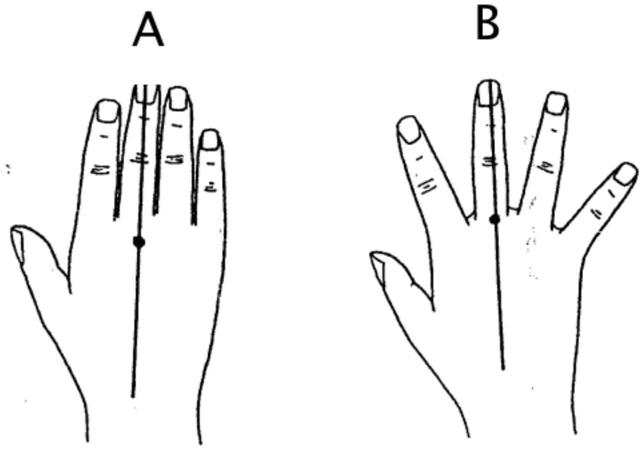

Figure 3.3: Finger Articulation : Abduction (A) : fingers moving towards each other, and Adduction (B) : fingers moving away from each other.

intermedial phalange, and the existence of the TMC (trapeziometacarpal) joint instead of the CMC joint in the finger structure.

TMC joint allows the opposition movement of the thumb.

Furthermore, the attachment of thumb to the wrist of the hand through the TMC joint allow the opposition action of the thumb. In contrast to the four finger anatomy, the thumb's TMC joint provides the abduction and adduction movement of the thumb, not the MCP joint. While, the IP and MCP joint has only 1DoF, allowing flexion and extension movements (Lippert [2011]). The thumb movements is demonstrated in figure 3.4.

Feature Points

feature points are used to track finger articulation and register the thumb on finger touch events, for interaction.

In this section, we describe the feature points which were used to create the separated planes origin points and from which we derived the axes for the plane coordinate system. These planes were later used to project the touch points on the respective phalanges and were computed relative to the phalanges plane origin points.

Similar to the hand kinematic model (Cobos et al. [2008])

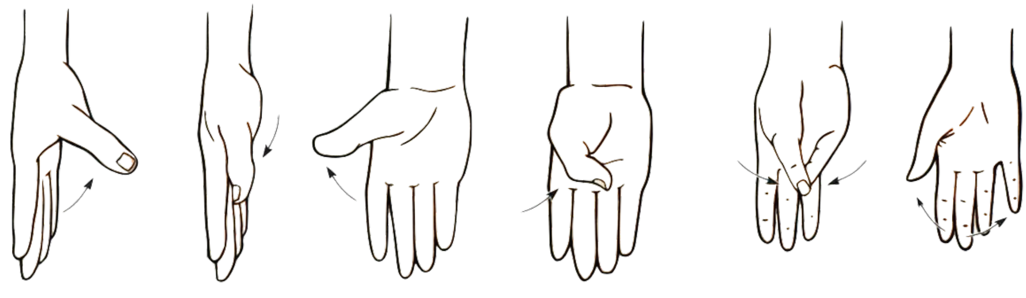

Figure 3.4: Hand Articulation : Types of articulations of the TMC, MCP and IP joints of the thumb.

and aforementioned anatomical structure of the thumb and finger, we used the joints motion and links between them to track our feature points and build the phalangeal planes coordinate system.

First, for each phalangeal plane, we have an origin point, and 3 axes for the 3 Dimensional plane (X,Y and Z). Demonstrated in figure 3.5, is the direction of the X and Y axis of the plane, and the red colour marks the origin of the plane.

Joints and fingertip are used as origin points, and the phalanges as independent 2D planes.

Due to limited DoF of the phalange movements aforementioned, we were able to derive the Y axis for the phalangeal planes of the same finger from the normalised vector computed between the MCP Joints of the different fingers. Furthermore, we used the computed Y axis, as the Y axis for the for the 3 phalange planes. For the index finger, the Y axis is computed from the normalised vector between MCP1 and MCP2 positions in 3D space, while the middle and ring fingers are computed from MCP2 and MCP3. Finally the pinky finger is computed from MCP3 and MCP4.

The Y axis of the phalangeal planes are created from the MCP joints of the fingers lying next to each other.

The choice of the MCP joints is due to the movement behaviour of the MCP joints and fingers during abduction and adduction movement (Lippert [2011]).

Furthermore, we derived the x-axis of the phalangeal planes by computing the normalised vectors between the different IP joints and MCP joint of the same finger, as follows :

Each phalange composed of a 2D plane with normalised x and y coordinate system.

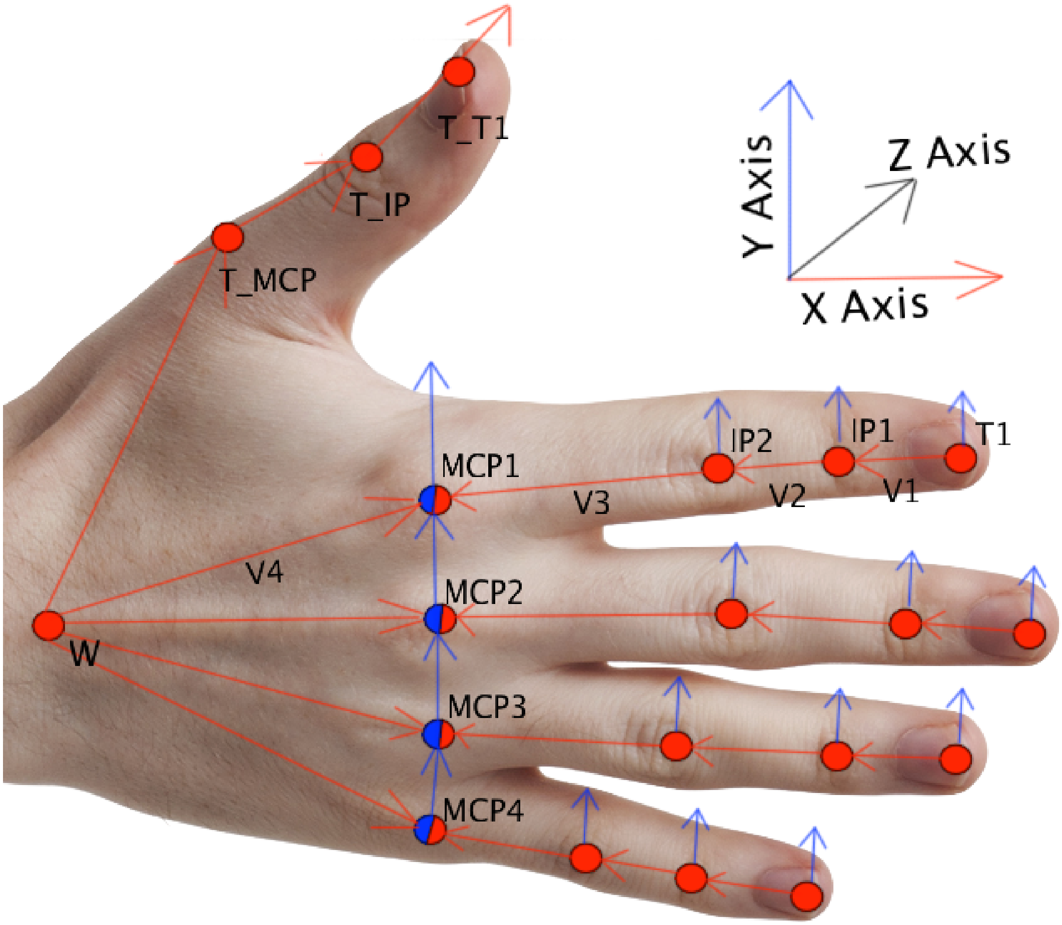

Figure 3.5: Feature Points : A labeled hand of the features tracked and used for touch events of the thumb on finger. Red/Blue markers represent MCP joints of the finger, and form which the Y axis of the phalangeal plane. Red markers represent the points of the IP joint and from which the x-axis of phalangeal plane

Distal phalange formed by the normalised vector ($\vec{V}1$) between the fingertip (T1) and DIP joint(IP1).

Intermedial phalange formed by normalised vector ($\vec{V}2$) between the DIP joint (IP1) and PIP joint(IP2).

Proximal phalange formed by normalised vector ($\vec{V}3$) between the PIP joint (IP2) and MCP joint.

Furthermore, the Z-axis of the phalange plane is computed using the cross product of the two normalised axis X and Y obtained above.

For each phalange plane also exists an origin point from which the points projected on this plane is in relative to :

Distal phalange origin point is the finger pulp flesh tip (T1).

Intermedial phalange origin point is the DIP joint (IP1).

Proximal phalange The proximal phalange, origin point is the PIP joint (IP2).

3.1.2 Finger Landmarks

Another characteristics of the hand is the landmarks and tactile features that are exhibited on the fingers, we classified these features into 3 categories, and used these classification later in the conceptual model in chapter 4 "User Study : The Conceptual Layout".

Tactile landmarks classified into fingertip, creases and middle bumps.

FingerTips

The fingertip exists on the extreme ends of the finger, they possess one of the highest concentration of touch receptors and thermo-receptors among all areas of the human skin. Each fingertip possesses more than 3,000 touch receptors, most of them are pressure sensors. they are densely packed under the skin,where they can report pressure events in overlapping fields of up to one tenth of an inch (Hancock [1996]).

Fingertip most sensitive for touch.

Skin Creases

The creases are the skin marks created by the bending at the IP joints locations. Therefore, the crease are referred to by the name of the joints, except for palmar digital crease. The palmar digital crease is created due to the flexion movement of the MCP joint, but it's not in the same location of the MCP joint.

Creases are skin folds on the finger and palm.

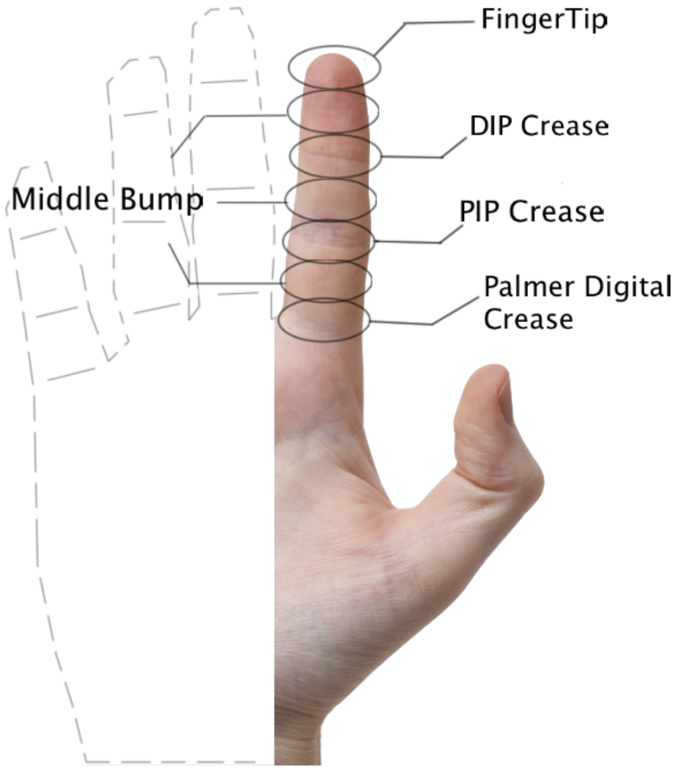

Figure 3.6: Finger Landmarks : A labeled hand model of the creases and other landmarks on the fingers.

Middle Bumps

Middle bumps is not an apparent landmark on the finger.

The middle bumps is not a apparent feature of the finger nor it is a medical term, but we used this term to describe the pulp flesh of the finger between two features.

Distal MiddleBump The pulp flesh between the finger tip and the DIP crease.

Intermedial MiddleBump The pulp flesh between the DIP crease and the PIP crease.

Proximal MiddleBump The pulp flesh between the PIP crease and the Palmer Digital crease..

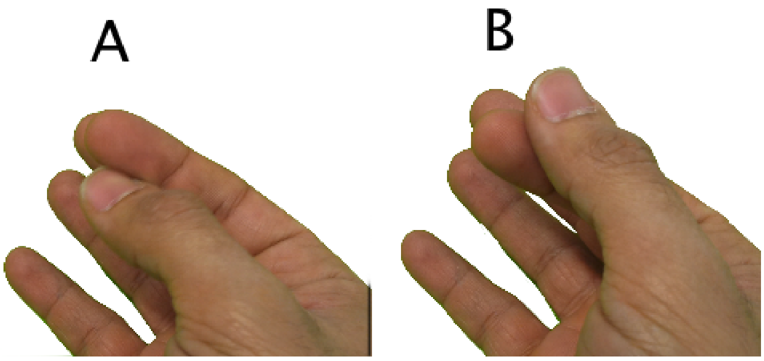

Figure 3.7: Finger Curvature : (A) Thumb touching the lower side of the finger (B) Thumb touching the upper side of the finger.

3.1.3 Finger Curvature

Another anatomical characteristics of the finger is it's semi-cylindrical shape. This shape infers the ability to touch different points across the width of the finger, rather than only across the length of the finger.

The semi-cylinderical shape of the finger, and DoF of the thumb allows touching the finger at different sides.

The wearable texting gloves such as Gauntlet (Liu [2012]) and KITTY (Mehring et al. [2004]) used the curvature of the fingers, and extended the contact points of their touch points to one side of the finger.

Furthermore, both gloves used the upper side of the finger, while we aimed to evaluate the effect of touch on both sides of the finger. We limit the selection on to the two extreme sides of the finger, the upper and lower finger as shown in figure 3.7. The limit of the two extreme sides of the finger was mainly due to feature tracking limitation, and to decrease the complexity of the touch layout to be tested later, in the user study.

3.1.4 Proprioception

Proprioceptors in the muscles & joints, allow sense of the relative positions of the hand, even with no visual sense.

A characteristics of the hand by which an individual can sense her relative position of the fingers and thumb and the strength employed in it's movement. It is provided by proprioceptors in the skeletal striated muscles and in the joints of the thumb and finger. This allows the thumb to know it's relative position from the fingers and phalanges, and also the fingers position from each other and the thumb Wikipedia [2003].

3.2 Mathematical Implementations

In this section, we demonstrate the mathematical formulas and transformations essential to our data analysis.

The feature points are used to (1) Select the appropriate phalange for projection of points (2) Projecting the 3D touch of the thumb on to the 2D phalangeal plane.

As we obtain the feature points mentioned in the hand anatomy section in 3 dimensional coordinate, we project the thumb 3D touch point on to the corresponding 2 dimensional position on the phalange plane.

Before calculating the 2D projection of the thumb on the plane defined by the two points at the end of each phalange, we need to identify which plane to project the thumb touch point on.

3.2.1 Phalange Selection

Using the same feature points discussed in section 3.1.1 "Feature Points" and figure 3.5, assuming each feature is a point in 3d space. we aim to obtain the phalange at which the thumb touch is upon, given the finger articulation.

First, we obtain the euclidean distance $|L3|$ between the fingertip (T1) and (MCP) joint 3d positions.

$$|L3| = \sqrt[2]{(T1_x - MCP_x)^2 + (T1_y - MCP_y)^2 + (T1_z - MCP_z)^2} \tag{3.1}$$

Furthermore, we obtain the euclidian distance $|X2|$ between MCP joint and the thumb fingertip (TT1)

$$|X2| = \sqrt[2]{(TT1_x - MCP_x)^2 + (TT1_y - MCP_y)^2 + (TT1_z - MCP_z)^2} \tag{3.2}$$

Finally, we obtain the distance $|X1|$ between thumb tip (TT1) and the fingertip (T1)

$$|X1| = \sqrt[2]{(TT1_x - T1_x)^2 + (TT1_y - T1_y)^2 + (TT1_z - T1_z)^2} \tag{3.3}$$

Using the Cosine Rule, and the distances obtained from 3.1, 3.2 and 3.6. We obtain α

$$\alpha = \arccos(\frac{X2 + L3 - X1}{2 * X2 * L3}) \tag{3.4}$$

After obtaining the angle α, we calculate the distance T from the fingertip (T1) to the perpendicular bisector of the thumb on the distance $|L3|$.

$$T = X1 * \sin(\alpha) \tag{3.5}$$

To compute L1, we calculate the euclidean distances $|A1|$ between T1 and IP1, and $|A2|$ between IP1 and MCP

$$|A1| = \sqrt[2]{(T1_x - IP1_x)^2 + (T1_y - IP1_y)^2 + (T1_z - IP1_z)^2} \tag{3.6}$$

$$|A2| = \sqrt[2]{(IP1_x - MCP_x)^2 + (IP1_y - MCP_y)^2 + (IP1_z - MCP_z)^2} \tag{3.7}$$

Using the Cosine Rule, again we compute α

$$\alpha = \arccos(\frac{A1 + L3 - A2}{2 * A1 * L3}) \tag{3.8}$$

Using Pythagorus, we obtain L1

$$L1 = A1 * \sin(\alpha) \tag{3.9}$$

Similarly we obtain $|L2|$, but instead of using IP1, we replace the IP1 with IP2. Finally, we check the T obtained

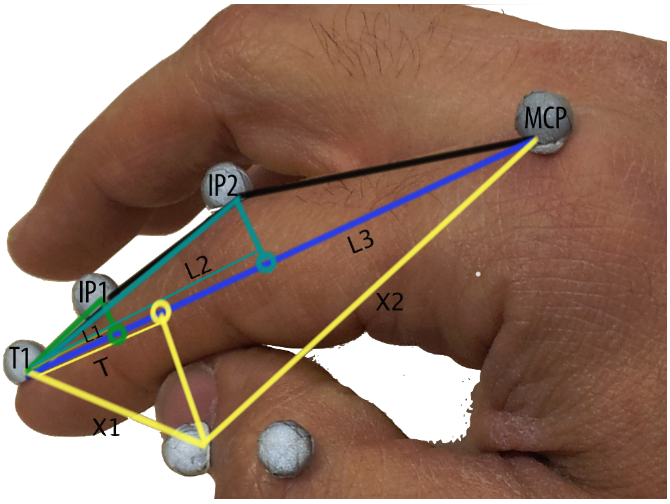

Figure 3.8: Mathematical : Using feature points and triangles to detect the location the thumb touch on the intended phalange.

from the thumb (TT1) distance in respect to the the fingertip(T1) and MCP joint, and between the distances $|L2|$ and $|L3|$ of IP1 and IP2 respectively, in respect to the fingertip (T1) and MCP joint.

Comparing the relative lengths of the joints and the thumb projection, to find intended phalange for the touch point.

Data: T, L1 and L2
Result: Selected Phalange
if $T \leq L1$ **then**
  return Distal Phalange;
else
  if $T \leq L2$ **then**
    return Intermedial Phalange;
  else
    return Proximal Phalange;
  end
end

Algorithm 1: Selecting phalange for projection

After selecting the appropriate phalange, we used this phalange coordinate system to project the thumb touch point as demonstrated in the coming section.

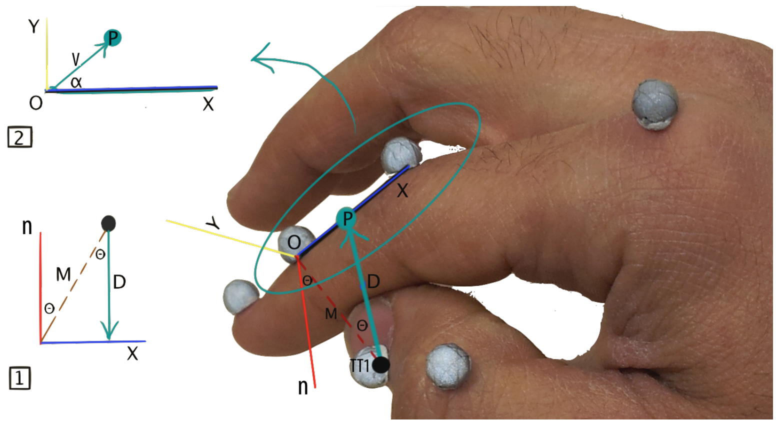

Figure 3.9: Mathematical : Stages of thumb touch on phalange projection (stage 1) projecting from tip of thumb to phalange (stage 2) calculate the new 2D coordinate position.

3.2.2 2D Projection of the touch points

Each phalange represent a plane on the finger with a point of origin (a feature point) [x0,y0,z0] and a normal [a,b,c]. While the touch point represented by the thumb [x1,y1,z1], as shown in figure 3.9

The projection of thumb touch point has 2 stages.

1. To obtain the Distance $|D|$ between the touch point and the phalange plane origin, and project the thumb touch point (P) onto the phalange plane (Stage 1) :

   (Stage 1) Project the thumb 3D touch along the normal of chosen phalange plane.

   (a) Computing the normalised vector $(\vec{M})$ between the thumb touch point (TT1) and origin (O).

   (b) Computing the angle (θ) between the $\vec{M}$ and the normal of the phalange $\vec{n}$

   $$\theta = acos(\vec{M} \cdot \vec{n}) \tag{3.10}$$

   (c) Computing the euclidian distance $|\vec{M}|$ between the thumb touch point (TT1) and origin (O).

   $$|\vec{M}| = \sqrt[2]{(TT1_x - O_x)^2 + (TT1_y - O_y)^2 + (TT1_z - O_z)^2} \tag{3.11}$$

(d) Then we obtain the distance $|D|$ needed by the thumb touch point (TT1) to move along the the normal of the plane in $\vec{Z}$

$$D = |\vec{M}| * cos(\theta) \tag{3.12}$$

(e) After computing the $|D|$, we obtain the projected thumb touch point (P) 3D position on to the phalangeal plane :

$$\vec{P} = TT1 - \vec{n} * D \tag{3.13}$$

(Stage 2) Compute new XY coordinate of the projected from the relative plane origin point.

2. After projecting the thumb touch point (P) on to plane, we obtain the vector (V) that is obtained from the difference between the origin point and projected thumb touch point (P). Afterwards we obtain the magnitude (mag) 3.14 and direction (nV) 3.15 of the vector (V). Then computing it's dot product with the X and Y axis of the phalangeal coordinate to transfer the point to the new XY coordinate system of the phalange.

$$|mag| = \sqrt[2]{(P_x - O_x)^2 + (P_y - O_y)^2 + (P_z - O_z)^2} \tag{3.14}$$

$$n\vec{V} = \frac{\vec{V}}{|\vec{V}|} \tag{3.15}$$

$$\theta_x = acos(n\vec{V} \cdot \vec{X}) \tag{3.16}$$

$$\theta_y = acos(n\vec{V} \cdot \vec{Y}) \tag{3.17}$$

The new XY coordinates of the thumb projected touch on the respective phalange.

$$X_{new} = |mag| * cos(\theta_x) \tag{3.18}$$

$$Y_{new} = |mag| * cos(\theta_y) \tag{3.19}$$

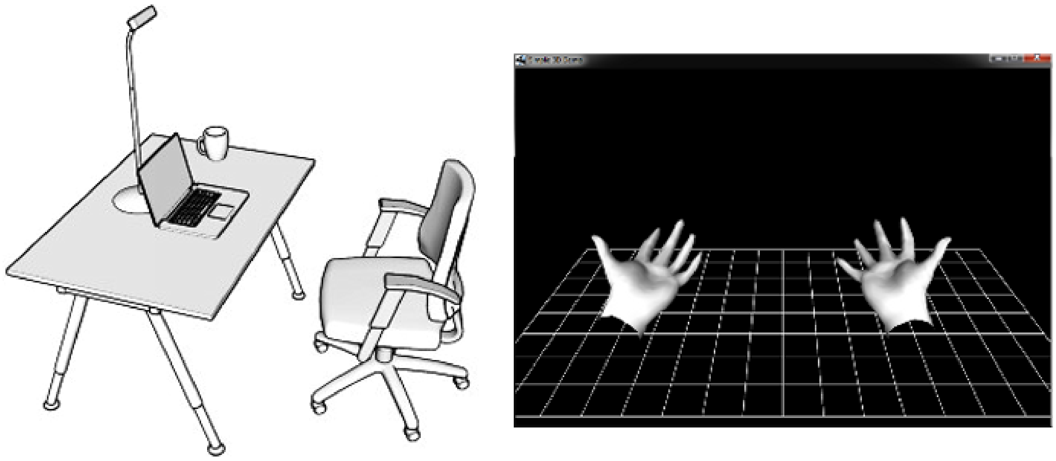

Figure 3.10: Instruments : (Left) The camera mount position for 3Gears systems (Right) The tracked hand software by 3Gears.

3.3 Instruments

In this section, we will demonstrate the instruments that was used to realise our concept, and used to attain the data needed for the analysis of the conceptual model. Both of our instruments were vision based systems, that tracked certain feature points in 3D space.

3.3.1 ThreeGear and Kinect

Our first prototype system based on the ThreeGear framework (3GearSystemsInc [2013]) and MS Kinect (Zhang [2012]). ThreeGear is a framework that enables 3D cameras to reconstruct the finger postures of the hand. 3Gears use inverse kinematics of the hand, which is derived from geometric methods e.g. the relation of triangles. The fingertips orientation and position is used to construct a chain of equation which calculate the rest of the hand joints and articulations (Cobos et al. [2008]).

3Gears is a framework to track the hand movements using inverse kinematics of the hand model

Based on a camera mounted above the desk, as shown in figure 3.10, the system captures the hand motion and gestures, and transfer the feature points such as the fingertips and joints of the hand into matrices of 3D positions and orientations. As mentioned in the hand anatomy section and implementation section, we used these feature points to compute the phalange plane and thumb touch point projection.

Software/Hardware Configuration

To calibrate the system, you need to spread out your fingers to find the correct scale model of your hands. The system will identify your hand scale to map it's hand model.

Advantages

1. No addition markers or devices needed to be attached to the hands
2. Calibration is simple and on the fly.
3. Realtime tracking of the hand features.

Disadvantages

1. The hand is a model based hand, the ratios between joints and phalanges are not real measurements, but a modelled one. For our user study this was a problem, as we needed the real lengths and real points to accurately measure the effectiveness and properties of our conceptual model.
2. Occlusion, as the thumb reaches for targets on the finger away from the tip, and for the fingers surrounded by other fingers such as the ring and middle. The fingers starts to occlude the thumb from the camera allowing lose of tracking in realtime, which cause data loss of these features.

1. No addition markers or devices needed to be attached to the hands

2. Calibration is simple and on the fly.

3. Realtime tracking of the hand features.

Implementation

In this section, we demonstrate the addition touch layer interface we added on 3Gears to detect and register a touch on the finger using the thumb.

1. Detection of the touch points on the respective finger and phalange using methods mentioned in section 3.2 "Mathematical Implementations" and 3.1.1 "Feature Points".

2. Using a distance threshold between the thumb fingertip and the phalange origin point (either tip or joint) to detect the touch occurrence.

3. Using a 1€ filter to smooth the data stream of the thumb 3D position, when computing the movement vector between thumb previous and current position, to detect when the thumb leaves the phalange and when it enters for touching. .

3.3.2 Vicon Nexus

Vicon is a motion tracking system, which is composed of infrared emitting and detecting cameras and a software which allows processing and tracking of the position and orientation of reflective markers in 3-dimensional coordinates.

The Vicon Nexus software allow the construction and tracking of dynamic models composed of groups of reflective markers, such as in our user study the human finger and thumb. This allows tracking arbitrary movements of the hand and finger in sub millimetre precision.

Vicon Nexus allows the construction and tracking of dynamic moving hand model.

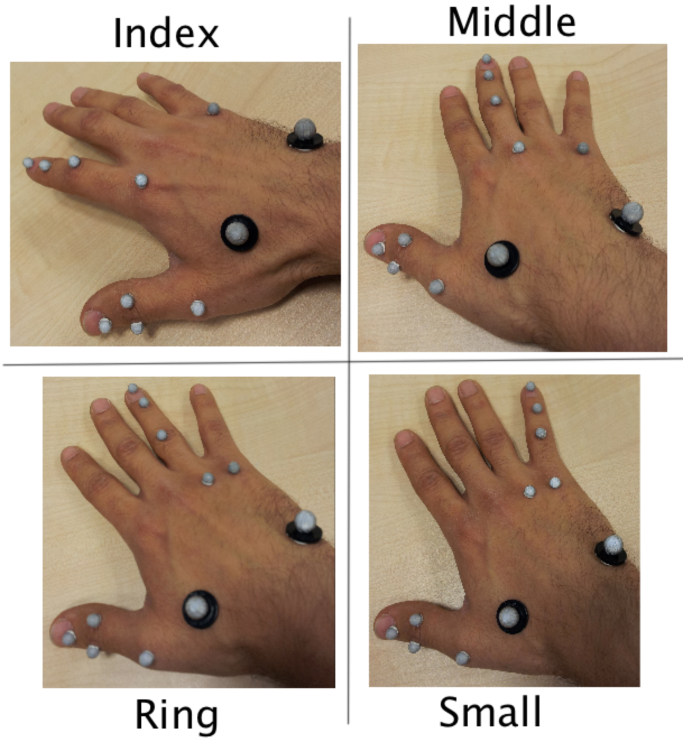

Figure 3.11: Instruments : The position markers which are fitted on the corresponding fingers of interest during the study.

As shown in figure 3.11, the markers are fitted on the joints and tips of the fingers in the same manner as described in the hand articulation feature points section. Using the Vicon Nexus software we record the session for offline processing, and filling the gaps of the lost marker positions during recording.

Software/Hardware Configuration

Calibration for the Vicon more time is needed, as the subject must be fitted by the physical markers, then a skeleton of the marker in the tracker database must be must be fitted virtually on the current model as seen in figure 3.12. Finally, the session can be recorded, and all subject's movement are recorded in 3 dimensional coordinates.

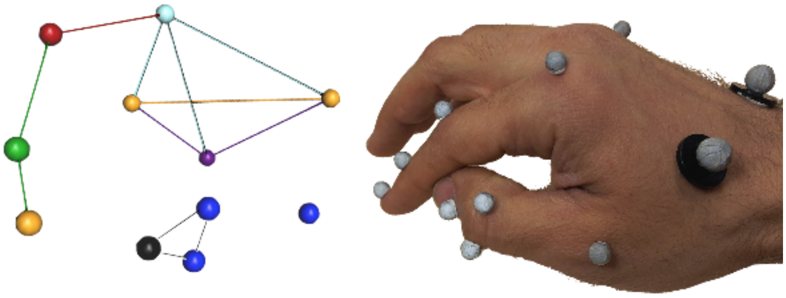

Figure 3.12: Instruments : (Left) Vicon Hand Skeleton in 3D space (Right) the markers on the hand mapping the Vicon Skeleton.

Advantages

1. The lengths and position of the markers reflects the real measure of the subject phalanges lengths and joints position, Rather than a computed model of the hand such as in ThreeGear.

2. Data is not lost, even if markers are occluded, it can be retrieved later from the recorded section, and the position of lost marker can be obtained from it's relation to the neighbouring markers.

Disadvantages

1. The system is not mobile, the cameras are stationary and must be calibrated once any camera's position changes.

2. Markers on the hand does not allow a real life application.

3. The procedure for calibration of the hand and finger is more tedious.

3.4 Conclusion

Vicon Nexus was used for millimetre accuracy evaluation of the touch precision of the thumb on finger interaction.

In conclusion, the Vicon Nexus system was used for obtaining the data necessary to measure our conceptual model effectiveness, precision and behaviour. As for the 3Gear implementation is rather a step towards a more practical implementation given that the depth cameras are getting smaller, and can allow a more mobile implementation.

Overall in this section we discussed the hand anatomy and it's effect on our user study, we demonstrated the calculation of our data points of interest that are used to measure our dependent variables, and finally the instruments used to capture these data. In the next chapter we will demonstrate the user study research questions, procedures, hypotheses and statistics and data correction.

Chapter 4

User Study : The Conceptual Layout

In this section, we discuss the aim and rationale of our conceptual layout, and the criteria we used to evaluate the independent variables. Furthermore, we will demonstrate the procedure and the method of evaluation of the our conceptual layout. Furthermore, the hardware and software configuration, methods of data correction and our result analysis.

4.1 Aim & Rationale

In this study we aim to evaluate the hand landmarks, curvature and proprioception for thumb on finger touch interaction, as mentioned in the design approach section 3.1 "Hand Anatomy & Characteristics". Similar to the work of Gustafson et al. [2013] and Dezfuli et al. [2012], we aim to evaluate the thumb touch over the finger in an eyes-free interaction.

Evaluate the thumb and finger interaction using time duration of selection, pain, hand posture and precision as metrics.

In reference to the characteristics of the hand mentioned in the hand anatomy section 3.1.2 "Finger Landmarks", we formulated a 9 target conceptual layout for theses touch targets, as shown in figure 4.1.

Figure 4.1: User Study : The 9 targets conceptual layout of the individual finger.

9 targets conceptual layout forms the single row condition.

The rationale behind this 9 touch targets conceptual layout is to use the creases tactile sense, to evaluate the ability of the creases to separate targets overlaid near the creases (targets 3,4,6,7). Moreover, evaluating the touch points on landmarks such as the tip of the finger (target 1), base of the finger (target 9) and middle bumps (targets 2,5,8).

Moreover, Overall, the concept is to have 3 targets per phalange per finger, to find out the optimal number of targets that can be laid out on each of the finger phalanges and the characteristics of these touch points.

9 targets conceptual layout extended to the sides of the finger, forming double row 16 target layout.

Furthermore, as the finger sides were used by implementations such as KITTY (Mehring et al. [2004]) and GAUNTLET (Liu [2012]). We extended the 9 target conceptual layout to the sides of the finger, formulating a 16 targets conceptual layout. Mainly the targets are distributed as two 9 targets layout, but on the upper and lower side of the finger, as shown in figure 4.2.

Similar to other eyes-free studies mentioned in 2.2 "Evaluating Eyes-Free Interaction & On-Body Landmark Effectiveness", participants in our user study were visually hindered from seeing their hands while asked to touch the targets of our 9 targets and 16 targets conceptual layouts.

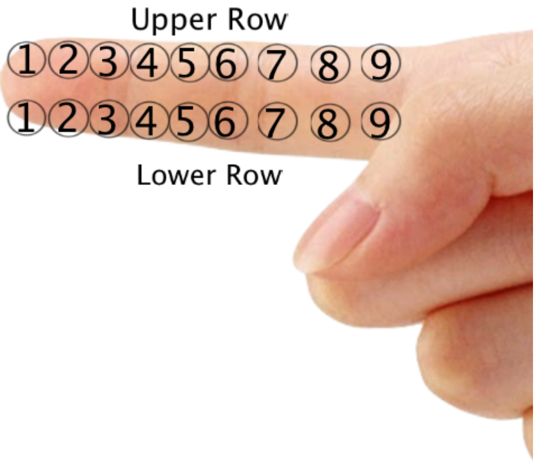

Figure 4.2: User Study : The 16 targets conceptual layout of the individual finger, with double rows condition (Upper and lower rows)

4.2 Experimental Design

In order to evaluate the 9 targets conceptual layout for the single and double row conditions, a within-subject user study was designed. Participants task was to perform mapping between visual stimuli shown on a screen, which is mainly targets highlighted on a virtual prop hand, and between the touching their finger using the thumb on finger.

Within-subject user study, evaluating two conditions(singe and double rows), for the four fingers.

Participants were visually occluded from their hands, hence removing their visual sense, and testing only their tactile and proprioceptive sense to find the required position to touch. Furthermore, we record the time for users to find and confirm the touch of these targets.

The confirmation of the target is implemented by allowing the subjects to use an external confirmation button, to confirm that they touched the required target displayed on the screen, on their finger. In order to move to the next target.

4.3 Independent Variables (IV)

Fingers and target condition order were balanced using a 4x4 and 2x2 latin square respectively.

The main independent variables are :

1. *Four Fingers* - Index, Middle, Ring and Pinky fingers.
2. *Touch Targets* - Targets labeled 1 to 9 as shown in figure 4.1.
3. *Targets Conditions* - Single Row and Double Row

The finger and target condition order were balanced among participants to compensate for any external influence such as fatigue of the hand, using a 4x4 latin square for the fingers and 2x2 for the conditions. The targets were assigned randomly per each chosen finger and condition.

Another categorial classification of the targets

Other Independent variables which are categorical factor of the targets :

1. *Landmarks* - Fingertip (Target 1), Creases (Targets 3,4,6,7), Middle bumps (Targets 2,5,8) and Finger base(Target 9).
2. *Phalanges* - Distal (Targets 1,2,3), Intermedial (Targets 4,5,6) and Proximal phalanges (Targets 7,8,9).

4.4 Dependent Variables (DV)

4.4.1 Targets Spread

Assuming the distribution of the (x,y) positions is a Gaussian distribution, we calculate the target mean (μ) and spread, which is double the standard deviation (2σ) and the number of data points(N) per target class of the normalised x & y positions.

Each of the equations (4.1) and (4.2) are applied to the x and y positions, each target separately.

$$\mu = \frac{1}{N}\sum_{i=1}^{n} x_i \tag{4.1}$$

$$\sigma = \sqrt{\frac{1}{N}\sum_{i=1}^{n}(x_i - \mu)^2} \tag{4.2}$$

The spread of the target is in a normalised form, Furthermore, if we need the real target size in millimetres, we compute the the normalised spread value by the average phalange length in millimetres.

4.4.2 Time of Selection

It's the time calculated from timestamps recorded between consecutive touches. This time represents the time taken between finding and selecting the required target using the confirmation button during a trial.

Selection time recorded in milliseconds.

The target is selected in random order 8 times through a trial. We calculate the average time taken across the 8 times.

4.4.3 Angle of Impact

Another observation in the pilot tests is how the thumb touch angle with the finger changes across targets. Mainly due to the physical properties of the joints and ligaments that attach the thumb to the hand, allow it's free movement in comparison to the finger as mentioned in section 3.1.1 "The Opposable Thumb".

The posture of the thumb when selecting target on the finger.

Therefore, we also computed the angle that the thumb makes when in impact with the finger, as shown in figure 4.3. The angle greater than or equal to 90 degrees indicates that the thumb tip touch the finger. Moreover, as the angle decreases, the finger is touched more by pad of the thumb, rather than the tip.

Thumb touch on finger can vary from using it's tip to the pulp flesh of it's distal phalange.

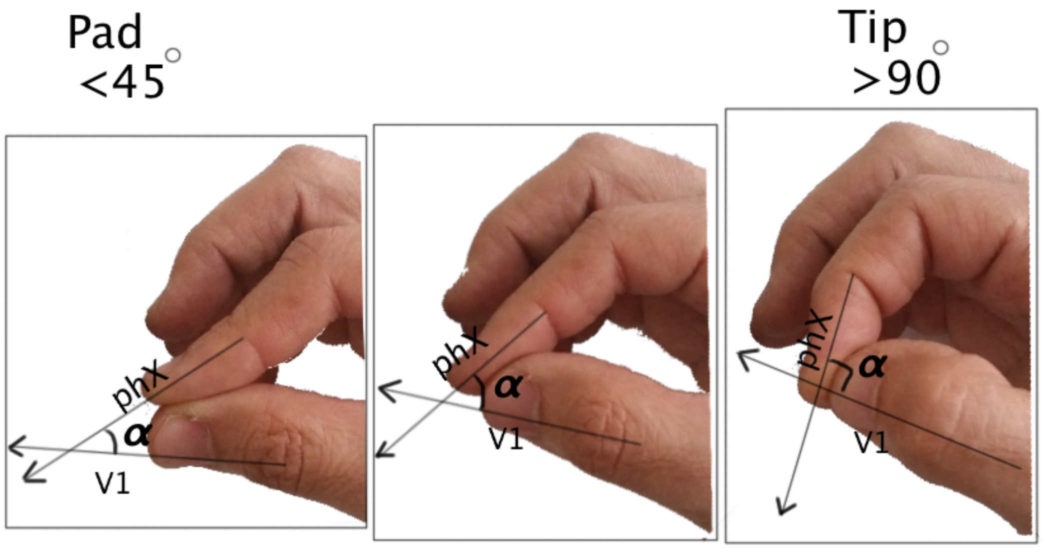

Figure 4.3: Impact Angle : Thumb touch orientation on finger from 90deg perpendicular to the touch point using thumb tip, up to less than 40deg to the touch target using the thumb pad.

1. Computing the normalised vector $\vec{V}1$ from the thumb tip and thumb proximal joint.
2. Calculating the dot product of $\vec{V}1$ and the selected phalange plane X-axis $ph\vec{X}$, and obtaining the angle using arc cosine of the dot product.

$$\alpha = acos(\vec{V}1 \cdot ph\vec{X}) \tag{4.3}$$

4.5 Hardware Configuration

Input : thumb on finger touch and spacebar to confirm, output : vertical display for stimuli and feedback.

The user study was executed on a standard desktop computer, with a 23 inch display screen where the visual stimuli for the participant is shown. The study was enclosed within a ridged aluminium structure, which hosted a set of IR capturing cameras and a motion tracking system (section 3.3.2 "Vicon Nexus").

Furthermore, participants were asked to put their hands on

Figure 4.4: User Study : Hardware experiment settings.

an arm rest while a blinder was used to separate the participants visual sense from their hand. Participants follow the visual stimuli displayed on the screen, as shown in figure 4.4.

The participants were fitted with infrared reflective markers as shown in figure 3.11. Moreover, markers were also fitted on the spacebar key of the keyboard which is used as the confirmation button. Participants use the spacebar to confirm the selection of the target. The session is also recorded using a GoPro camera during the study, .

4.6 Software Configuration

An application was designed to display a yellow highlight

a touch-and-confirm task, require participants to touch

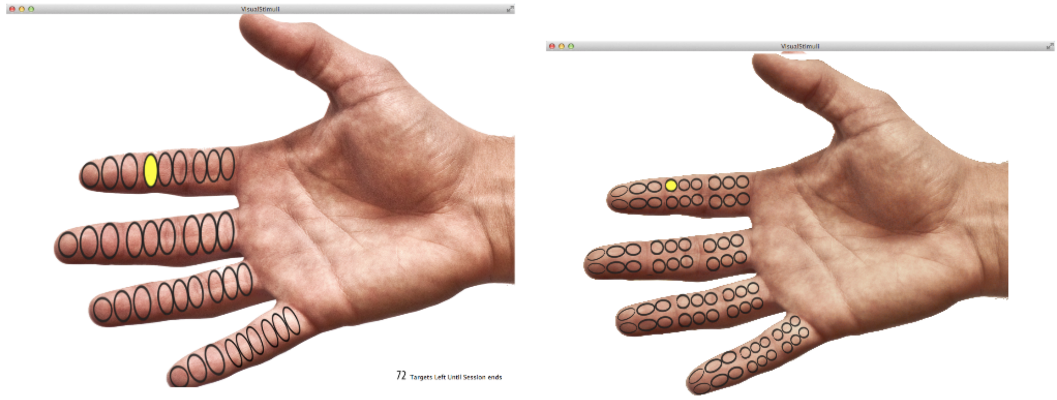

Figure 4.5: User Study : (Right) the single row, 9 target conceptual layout and (Left) the double row, 16 targets conceptual layout with random highlighted target as visual stimuli for the participant .

their finger and confirm selection, to complete trial.

on a virtual hand shown to the subjects, as demonstrated in figure 4.5. The subject is required to do *a touch-and-confirm task* , in which after the target is highlighted, the subject is required to touch the target on their finger and press the spacebar as a means of confirming her selection to move to the next randomly displayed target.

The preprocessing is divided into two parts. First, the offline capturing of the finger motion is done using the Vicon motion capturing software, while recording the timestamp and sequence of visual stimuli shown to the participants after each confirmation button press.

In the second phase, we synchronise the data from both systems to extract the XYZ positions of the hand at which the touch point confirmation occurred.

4.6.1 Offline Recording

a vicon sync marker on the spacebar used for synchronise between two domains.

The data is stored on two systems. First, the participant recorded sessions of the 3D motion on the Vicon Nexus during the study, which is exported as a CSV file for data logging. The file contains the frame number, and the XYZ position values of all the markers shown in figure 3.12.

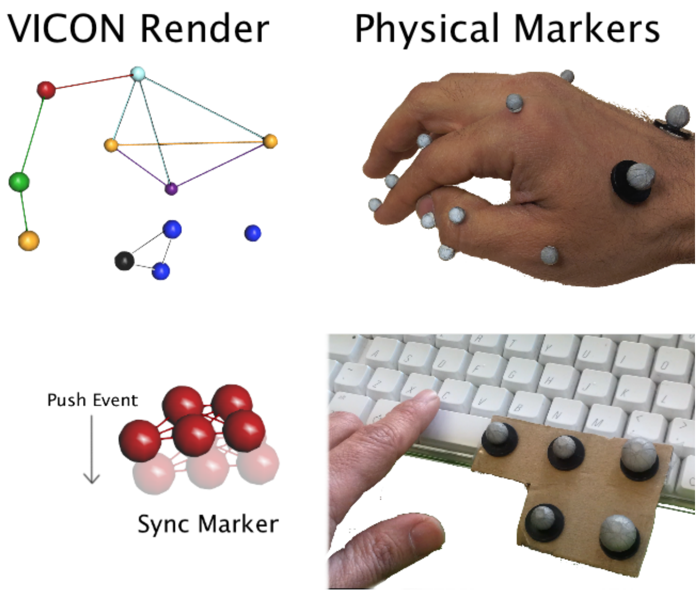

Figure 4.6: User Study : (Top Right) Rendered finger/thumb layout (Top Left) Phyiscal Markers on hand (Button Right) Rendered sync marker (Buttom Left) Physical Markers on confirmation button.

Second, the hand stimuli software which displays the random target for the users to select, and store the timestamp at which the target was selected and the random target identity in an CSV also for data logging. Finally, to extract the correct frame from the Vicon data, at which the target was selected, we used a *sync marker*.

4.6.2 Extraction & Synchronisation

As shown in figure 4.6, the IR sync marker attached to the spacebar ensures that we are able to mark and synchronise the Vicon frames with the time and target Identification at which the participants confirmed her touch and move to the next target, by pressing the spacebar.

sync marker is constraint to only move in the z-direction of Vicon space.

Extraction occurs by tracking the sync marker value change along it's z-axis in the Vicon 3D space. The spacebar key press detected by decrease in the z-value, and in the key re-

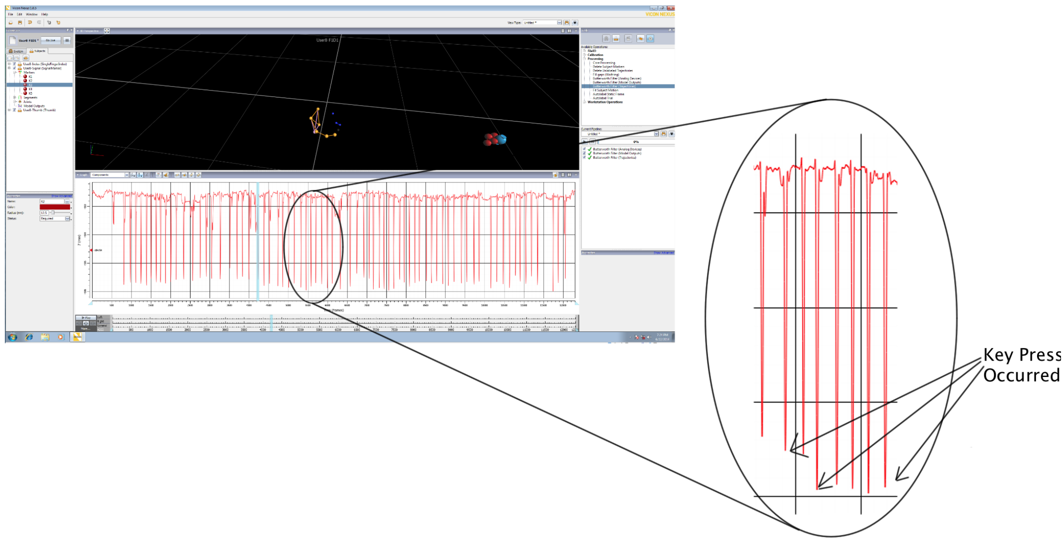

Figure 4.7: User Study : Vicon Nexus software interface (upper layer) 3D perspective view of the markers position and (Upper layer) motion graph.

the spacebar hit press down event is identified by a rate of change of values in z-axis equal to zero.

lease the z-value increases, as seen in figure 4.7. The frame is marked when the z-value reaches or surpass a minimum threshold. The current and next frame z-values are checked until the z-value of the current frame is lower than the z-value of the next frame, this indicates the end of the key press phase. We capture the touch event frame at the end of the key press and before the start of the release phase.

4.6.3 Data Processing

Phalange lengths per finger per participant is pre-measured and used for normalisation of data points.

After extraction phase and synchronisation, we compute the 2D projected positions, the time of selection and the target at which the touch was intended for, including the target number (1-9) and the finger. Furthermore, the normalised 2D position is computed from the pre-measured participants four finger phalanges. we input these lengths before exporting the final CSV file, which we used to perform our analysis.

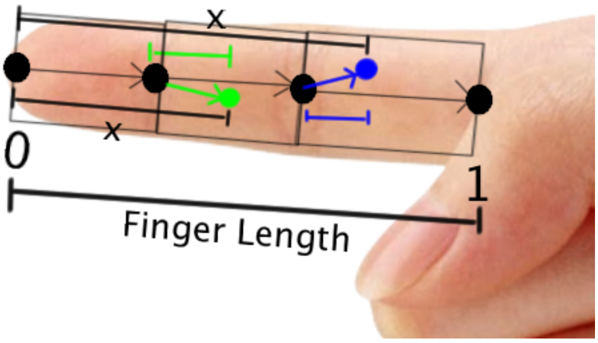

Figure 4.8: User Study : The normalisation of the point in x-value by finger length and phalange.

4.6.4 Normalisation of Data Points

The main dependent variable, from which we derive the targets mean and spread, is the projected thumb touch point (x,y) position. These values are obtained using the calculations mentioned in section 3.2.2 "2D Projection of the touch points".

X-Position

The x-position data points are normalised using the finger length of the corresponding finger of each participant. This allows us to compare the relative positions of the targets per phalange across different participants whom have different phalange lengths per finger.

X-positions are normalised using the finger length per finger per subject.

Furthermore, the reference point used for normalisation is the tip of the finger. The data point is normalised using the knowledge of which phalange it was intended for the touch and the relative x position point calculated from the projected point in reference to this phalange.

As demonstrated in figure 4.8, The final data point value (x) after projection is computed by adding the length of the previous phalanges to the x-position value of the touch on the intended phalange. Finally data point is normalised on the finger length.

Y-Position

Y-positions are normalised using the maximum and minimum recorded value per target, per finger per subject.

While for the y-positions, due to the observed inconsistencies of the finger's width across the finger length from tip to base. We normalised the target's y-position per participant, per finger by obtaining the maximum and minimum recorded value of y-position per target per finger per participant, afterwards we normalised each y-value using equation (4.4).

$$\frac{Y\,Value - miniValue}{maxValue - minValue} \tag{4.4}$$

4.7 Experimental Procedure

For each participant, the experiment procedure was as follows :

1. Participants were provided with an explanation of the task to be performed, and were requested to sign a consent form.

2. Participants phalanges on different finger are measured in millimetres.

3. A training phase was conducted to allow users to get acquainted with the touch and confirm technique, and to get acquainted with the double rows touch point condition.

4. Once training was completed, the participants performed trials of the touch-and-confirm task for each finger and condition (single row and double rows) in a separate trial. Fingers were selected using a 4x4 latin square, while the conditions were selected using 2x2 latin square .

5. Each trial is separated by a short break, in which users were asked about qualitative opinions concerning the touch points.

4.8 Participants

The sum of 4 participants, 3 male and 1 female were recruited. All participants were right-handed with an average age of 25.25 years and students at the local campus at RWTH Aachen. The order of tasks was balanced among participants, to prevent any influence of learning or exhaustion.

4.9 Statistical Methods

The within-subject design of the user study is 9 targets, 3 fingers and 2 layout conditions (single and double rows condition). For the double rows layout, there are 2 target conditions (upper and lower row). Furthermore, the analysis of landmarks spread was also in which are groups of targets combined and classified in 4 categories as mentioned in section 4.3 "Independent Variables (IV)" were used instead of the individual targets.

ANOVA used for analysis of targets per finger per condition.

Analysis of variance (ANOVA) was performed on 9 different groups of targets per each finger, per each target condition to quantitatively analyse the touch points as explained in section 4.6.4 "Normalisation of Data Points" and impact angle difference among the groups mean and variance. Benferroni correction was used to counteract the problem of multiple comparisons with anova, and to avoid type I errors of rejecting the null hypotheses when it's true.

post-hoc test to analyse effect levels and patterns.

Furthermore, Tukey's post-hoc test was used to analysis the effect level of each of these targets on each other, hence to find patterns between the targets and fingers, and their effect on each other.

4.10 Outliers & Data Correction

Outliers were removed through two phases :

4.10.1 Video Annotation

Videos used to mark participants behavioural faults on certain points.

Targets which fall outside the bound of it's intended phalange normalised range e.g. a point at the distal phalange which surpassed 1 or below 0, are considered potential outliers. For each of these points, the timestamp of the target at video of the recorded session was viewed, and the movement of the finger is observed.

The target is declared a fault, if it was indicated by the participant, that it was not the intended target after the touch point occurred. During the trial session, some participants declared after they touch and confirmed the target, which was not their intended choice.

Furthermore, targets in which participant mistakenly watched their hands while touching and confirming the targets were flagged as user faults and were also removed.

4.10.2 Interquartile Range

IQR is used to detect outliers in data points in a gaussian distribution.

Furthermore, The interquartile range(IQR) bounds was used to remove further outliers, after the video annotation. The interquartile range calculated from data points per each target per finger, per participant. The IQR tells how spread out the "middle" values of your data, and it can also be used to tell when some of the other values are "too far" from the central value. These "too far away" points are called "outliers" (Stapel [2014])

After computing the median of the 50th percentile, splitting data into two halves. The median of the first half "25 percentile" (Q1) is calculated, and the median of second half "75 percentile" (Q3) of the data is calculated. Finally, the IQR is calculated using equation 4.5

$$IQR = Q1 - Q3 \tag{4.5}$$

Furthermore, the higher and lower bound of the data is computed using the equation 4.6 and 4.7. Data points outside these bounds are labeled as outliers.

$$HigherBound = Q3 + (1.5) * IQR \tag{4.6}$$

$$LowerBound = Q1 - (1.5) * IQR \tag{4.7}$$

4.11 Qualitative Analysis

From the observations of the video, and interviews between trials, two issues were noticed :

4.11.1 Hand Posture

Participants were not guided to assume a certain hand posture.

Participants during the sessions were not guided to how they should touch these targets using their thumb. Nevertheless, it was noticed during the sessions, there were two main different hand postures during thumb interaction. These change in postures may affect the tracking techniques of the hand, and implementations.

Postures were classified into two categories.

As shown in figure 4.9, in the first posture subjects move their finger towards their thumb. In this posture, the finger articulates and moves until it reaches the thumb or both the thumb and fingers reach half ways. This technique is similar to the the concept on which KITTY (Mehring et al. [2004]) was developed upon, as the fingers where used to touch over the thumb.

On the other hand, one subject used his thumb to reach for the fingers, by containing his fingers into a ridged plane and forced the thumb to move and touch over the fingers, Similar to the implementation concept of PinchWatch mentioned in section 2.3 “Implementations & Existing Technologies”.

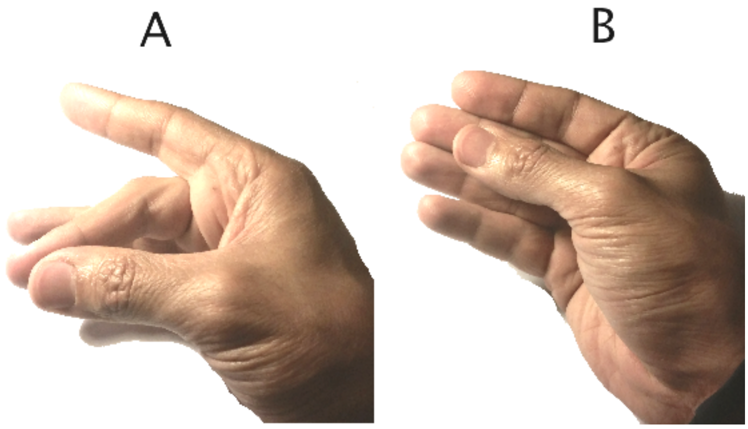

Figure 4.9: Qualitative Analysis : Hand postures (A) Finger touching thumb technique, (B) Thumb touch finger technique.

Furthermore, another observation was the target localisation strategy. The videos revealed that most subjects in their searching mode for the target were able to use the crease as a stopping mechanism. Furthermore, for locating targets near the creases, subjects tend to stop on the crease and then feel their way slowly before and after the crease to reach the required targets.

The selection process of the middle bump although contain more movements, yet the motion seem faster than selection near the creases.

While for the middle bumps, subjects tend to drag their fingers across the phalange alternating between the two crease to identify the middle bump. Furthermore, this alternation of the thumb between the creases seemed to be done faster than feeling targets before and after the creases. Finally, the tip(1) and base(9) of the finger were identified faster than all other targets.

Time of selection will be investigate thoroughly in section 4.12.1 "Selection Time Analysis". Nevertheless, through all the videos of the different fingers of the subjects, it was observed that there was no distinct difference between fingers.

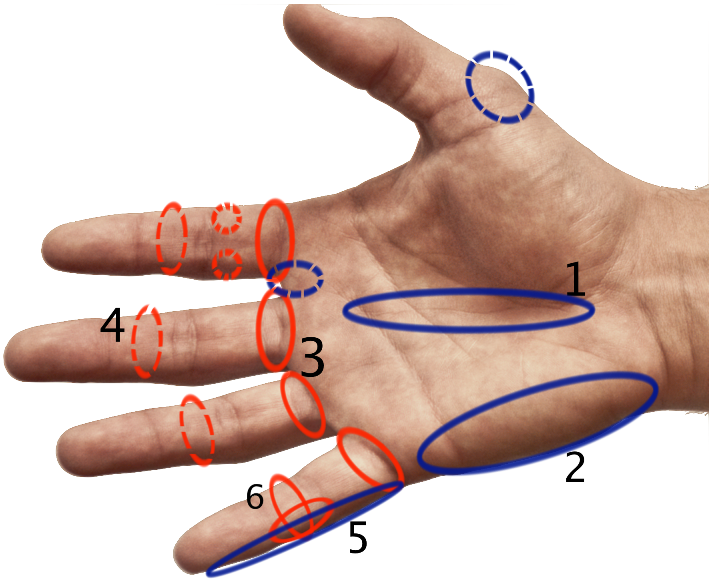

Figure 4.10: Qualitative Analysis : Discomfort diagram on the prop hand, dashed circles for conditional discomfort, while solid line for persistent discomfort.

4.11.2 Discomfort and Pain

At the end of each trial during the user study, a follow up interview is conducted to discuss the participants selection experience. Difficulty or annoying targets are reported. Furthermore, we allow them to mark the locations of discomfort and pain on a prop hand printed on a sheet. Pain and annoyance location on the hand is reported, and the level of irritation or discomfort.

Pain and annoyance are measured qualitatively.

As shown in figure 4.10, subjects were asked to mark areas which was discomforting or in pain. The red dashed line in the figure demonstrate a conditional discomfort which occurred among a single subject, while the solid line demonstrates a persistent discomfort in which all subjects reported. Moreover, the blue line marks the pain experienced during selection.

Areas causing discomfort and pain were marked on a hand diagram.

Mostly all male subjects had this persistent pain or cramps in the area around the *Palmaris Longus* muscle marked as

Male participants noted pain in areas in the centre of the palm, while female subjects did not.

(1) in figure 4.10. While the most discomfort and pain were due to the small finger targets, as they cause direct pain in the muscles and tendons marked in areas (2) and (5). While, female participants did not report this kind of pain.

4.11.3 Implication

Targets on the proximal phalange estimated to have the worst precision.

Finally, the results of the prop hand markings allowed us to build a preliminary hypotheses concerning the quantitative analysis for the precision of the touch targets. Moreover, we lead to believe that targets near the proximal phalange marked as areas (3) of each finger will have the worst precision of touch. While only a single subject complained of the middle bump targets, we believe the middle bump targets were identified successfully by participants.

Double row condition was perceived more hard than single row for targets on proximal phalange.

Finally, it was observed that overuse of the thumb over finger interaction caused fatigues located around the *Flexor digiti minimi brevis* and *Palmaris Longus* muscles, (Healthline [2005]) which are the deep muscles existing around the marked areas (1) and (2). In our study, participants had to perform 800 touch for the target conditions (single and double rows) and the 4 fingers. While most subjects felt more relaxed during the single row condition over the double row. The double row was perceived more difficult specially for targets on the lower proximal phalange, which are marked as areas (3).

4.12 Quantitive Analysis

Furthermore, the touch data points from our previous user study were gathered, and statistical analysis was run to find significants and to compute the touch precision, time duration and the range and significants of the impact angle. Data points in this analysis is for only 3 fingers (index middle and ring).

4.12.1 Selection Time Analysis

Q1. How much time does it take to select and confirm a target on the finger using the thumb, given different characteristics of the hand and finger ? hmm

The hypotheses that are constructed from our observations, as discussed in the qualitative analysis :

H1:
Targets on the tip (1) and base (9) of the finger will be the fastest, while the middle bump (2,5,8) will be second slowest. Finally, the creases (3,4,6,7) are the slowest.

Hypothesis: *H1*

H2:
There is no significant difference in time of selection and confirmation between same targets of the different finger.

Hypothesis: *H2*

H3:
There is no significant difference in time of selection and confirmation between same targets of the same fingers in different Target conditions.

Hypothesis: *H3*

Source	DF	DFDen	F Ratio	Prob >F
Target	8	2473	13.8352	<.0001*
Finger*Target	16	2473	1.4573	0.1066
Finger*Target Condition*Target	32	2473	0.8892	0.6462

Table 4.1: Time Analysis : ANOVA with Bonferroni correction results for time of selection. 'Targets' showed significant effect on results.

Time of selection was measured in seconds, ANOVA with Bonferroni correction (table 4.1) revealed that the targets had a main effect ($F_{(8,2473)} = 13.8352$, $p < 0.0001$), moreover, there was no significance in the interaction effect between the fingers and target condition. Tukey's post-hoc test (table 4.2) showed that the significant effect of the targets was due to the tip (target 1). While targets 2 and 9 has not statistically significance from the rest of the targets, nevertheless they are still 2nd and 3rd fastest targets.

The targets only had the main effect on the time of selection across all fingers.

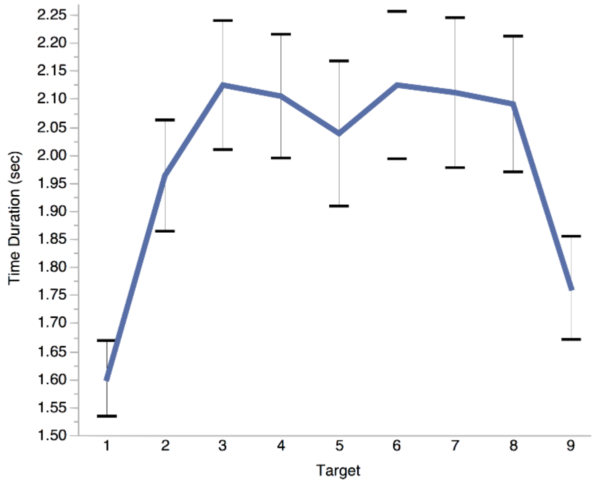

Target	Mean	Lower 95%	Upper 95%
1	1.60126	1.4926170	1.7132649
2	1.96284	1.8555474	2.0757003
3	2.12425	2.0143024	2.2371617
4	2.10450	2.0024564	2.2270610
5	2.03795	1.9330700	2.1566222
6	2.12428	2.0180255	2.2409236
7	2.11088	2.0065330	2.2280595
8	2.09052	1.9836446	2.2076120
9	1.76272	1.6798673	1.9077520

Figure 4.11: Time Analysis : Targets mean time and 95% confidence interval

Fingers and target condition (double or single) had no effect on time, H2 and H3 confirmed.

Furthermore, hypotheses H2 and H3 has been confirmed, which allows us to calculate an averaged timing per target for all 3 fingers and target conditions.

Level				Least Sq Mean
4	A			2.1481921
6	A			2.1461414
7	A			2.1442892
3	A			2.1422168
8	A			2.1123637
5	A			2.0591081
2	A	B		1.9885498
9		B	C	1.7919924
1			C	1.5899824

Table 4.2: Time Analysis : Tukey's post-hoc test results for the time of selection. 'Targets' 1 and 9 showed a distinctive effect.

The average timing for searching and confirming a target is 2 seconds. As demonstrated in figure 4.12, Furthermore,the timed needed for the searching method mentioned in the qualitative analysis, of the targets near the creases (targets 3,4,6 and 7) had no significant different than the targets on the middle bumps (targets 2,5 and 8) as demonstrated in

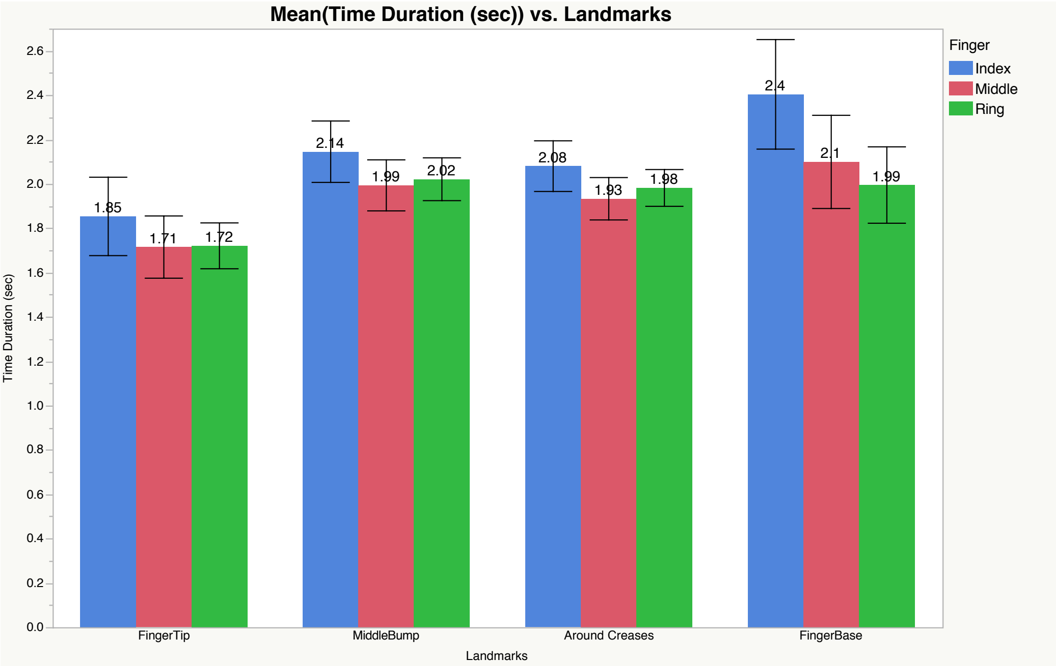

Figure 4.12: Time Analysis : Time of Selection of targets per finger and condition (single and double row).

table 4.2 and figure 4.11.

Nevertheless, the time need for selection on the middle bump varies for each phalange, but the variation was no significant. The middle bump on the distal phalange (target 2) had a faster mean time of 1.98 seconds, while for the target on the proximal phalange (target 5) it was 2.06 seconds. Finally the target on the proximal phalange (target 8) it was 2.11 seconds. Targets on the middle bump overall had an average of 2.05 seconds per touch.

No significant differences between timing of targets near the creases and middle bumps.

4.12.2 Touch Point Analysis

Q. (1)Are the 9 targets distinguishable on the different fingers, and (2) how precious are these targets given the different tactile nature of the targets, for both double rows and single row conditions ? we evaluated the question using analysis of variance (ANOVA), spread of the touch targets and the distance of the target mean centroid from it's neighboring targets.

Single Row Condition

Targets and fingers had significant effect on the touch points along the finger length.

ANOVA with Bonferroni correction demonstrated in table 4.3, for the normalised x-positions (section 4.6.4), showed that the target ($F_{8,821} = 3962.207, p < 0.0001$) had a significant effect on the touch points, also the fingers ($F_{2,821} = 8.3537, p = 0.0003$) showed a significant effect on the touch points.

Source	DF	DFDen	F Ratio	Prob >F
Target	8	821	3962.207	<.0001
Finger	2	821	8.3537	0.0003
Target*Finger	16	821	2.1495	0.0055

Table 4.3: Touch Point Analysis : ANOVA with Bonferroni results of touch point x-position for single row condition. 'Targets' and 'fingers' showed significant effect on results.

Level			Least Sq Mean
Index	A		-0.1363385
Middle	A		-0.1394451
Ring		B	-0.1821764

Table 4.4: Touch Point Analysis : Tukey's post-hoc test on fingers, for single row condition.

Finger significant effect was due to the ring finger, while all targets were significantly different on the fingers.

Tukey's post-hoc test showed that the significant effect of the fingers was due to the ring finger, as the effect level of the index and middle fingers were in the same level, demonstrated in table 4.4. We believe that this was due to the strict movement of the thumb movement on the index and middle fingers, compared to the ring finger. Nevertheless, we could not validate this assumption while missing the small finger in our analysis. Furthmore, Tukey's post-hoc test showed the effect of targets to be distinguishable and similar in all 3 fingers, as demonstrated in table A.7.

Double Rows Condition

While, ANOVA with Bonferroni correction for the double rows condition, as in table 4.5, revealed that the target ($F_{8,1649} = 5515.962, p < 0.0001$) had a significant effect on the x-position of the touch points, also the fingers ($F_{2,1649} = 17.0735, p < 0.0001$) showed a significance, while there was no significant interaction effect between the targets and the target condition (upper and lower).

Some of the targets in double rows condition were less distinguishable than the single row.

Source	DF	DFDen	F Ratio	Prob >F
Target	8	1649	5515.962	<.0001
Target Condition*Target	8	1649	1.1688	0.3143
Finger	2	1649	17.0735	<.0001
Target Condition*Target*Finger	16	1649	2.3338	0.0020

Table 4.5: Touch Point Analysis : ANOVA with Bonferroni results of touch point x-position for double rows condition. 'Targets' and 'fingers' showed significant effect on results.

Tukey post-hoc test as demonstrated in tables A.8, A.9 and A.10 showed that not all targets were significantly different. For the index finger upper condition , targets 5 and 6 were not distinguishable. While for the lower condition, targets 7,8 and 9 on the proximal phalange were not distinguishable.

Furthermore, the middle finger upper condition, targets 7,8 and 9 on the proximal phalange were undistinguishable. While, for the lower condition, only targets 7 and 8 were undistinguishable. Finally, the ring finger, for both the upper and lower finger, targets 7 and 8 were indistinguishable.

Furthermore, for the targets normalised y-positions, ANOVA revealed that the target conditions upper and lower targets ($F_{1,1649} = 2917.682, p < 0.0001$) have a significant effect, while there was no interaction effect between targets and target conditions.

The upper and lowers rows across the finger width were significantly different.

In conclusion, the results of the post-hoc test and ANOVA revealed that targets in x-position for the single row were all distinguishable with different effect levels, while for the double rows condition not all targets were distinguishable. Furthermore, the upper and lower targets y-position for

Participants were able to distinguish between most of the targets in both target conditions.

the double rows condition were also distinguishable by the participants. For the next section, we will demonstrate the precision of these targets and the imaginary button size revealed from the touch points spread.

Target Spread

The spread was calculated by doubling the standard deviation of the points.

We evaluated the spread of the targets for each finger, and the effect of the tactile characteristics (Fingertip, middle bump and creases) on the spread, similar to the affect of time aforementioned. Our criteria for evaluation is the larger the spread, the less accurate the target touch. While the lesser the spread, more accurate the touch. Furthermore, we evaluated how the same targets spread behave across the different fingers.

Hypothesis: *H1*

H1:
Targets on the tip and base of the finger will have the least spread, while the targets around the creases will be have the second least spread. Finally, targets on the middle bumps will have the highest spread, across all fingers.

Landmarks has a significant effect on the touch point spread.

Targets were classified as fingertip, finger base, around the creases and middle bumps. Moreover, as demonstrated in table 4.6, ANOVA was ran on the spread of the targets belonging to one landmark category as described in section 4.3 "Independent Variables (IV)", per fingers and target condition (double rows and single row). It was revealed that the significant difference in the touch point spread was due to the targets landmarks ($F_{3,189} = 5.1133, p = 0.002$), the fingers ($F_{2,189} = 14.3950, p < 0.0001$), and target condition ($F_{1,189} = 46.4080, p < 0.0001$). Furthermore, there was also revealed an interaction effect between finger and landmarks ($F_{6,189} = 4.6739, p = 0.0002$).

Targets on the middle bumps had no significant difference in spread from targets near the creases, or finger base.

Tukey's post-hoc test (table 4.7) showed that the finger tip and base had the same effect level, while the near creases targets had different effect levels from the fingertip and base. H1 was partially confirmed, as demonstrated in fig-

Source	DF	DFDen	F Ratio	Prob >F
Finger	2	189	14.3950	<.0001*
Landmarks	3	189	5.1133	0.0020*
Target Condition	1	189	46.4080	<.0001
Finger*Landmarks	6	189	4.6739	0.0002
Finger*Target Condition	2	189	1.9516	0.1449
Landmarks*Target Condition	3	189	1.5273	0.2088
Finger*Landmarks*Target Condition	6	189	1.4000	0.2166

Table 4.6: Landmark Analysis : ANOVA with Bonferroni correction results of touch point spread for single row and double rows condition. 'Landmark' showed significant effect on results.

Level			Least Sq Mean
Around Creases	A		0.04238014
MiddleBump	A	B	0.03973893
FingerBase		B	0.03425005
FingerTip		B	0.03177655

Table 4.7: Landmark Analysis : Tukey's post-hoc test results for the touch point spread for single row and double rows condition and Landmarks.

ure 4.13, the spread of the targets at the tip and base of the fingers were minimal, while the spread of the targets on middle bump was smaller than the targets near the creases. Moreover, The effect was not consistent across the 3 fingers as shown in table 4.8, as this interaction effect was due to the finger base (target 9) different effect level on the index finger in comparison to the middle and ring.

H2:
We assume all the same targets will have the same spread across all fingers, for both target conditions.

Null Hypothesis: *H2*

H3:
We assume the same targets will have the same spread across the upper row and lower row of the double rows condition.

Null Hypothesis: *H3*

Finger	Landmark						Least Sq Mean
Index	Around Creases	A	B				0.04596689
Middle	Around Creases	A	B	C			0.04224200
Ring	Around Creases		B	C	D		0.03893154
Index	FingerBase	A					0.05910353
Middle	FingerBase				D	E	0.02384529
Ring	FingerBase					E	0.01980133
Index	FingerTip		B	C	D	E	0.03220740
Middle	FingerTip		B	C	D	E	0.03627703
Ring	FingerTip			C	D	E	0.02684521
Index	MiddleBump	A	B	C			0.04301528
Middle	MiddleBump		B	C	D		0.03977260
Ring	MiddleBump		B	C	D	E	0.03642892

Table 4.8: Landmark Analysis : Tukey's post-hoc test results for interaction effect between the landmarks and fingers touch point spread for single row and double rows conditions.

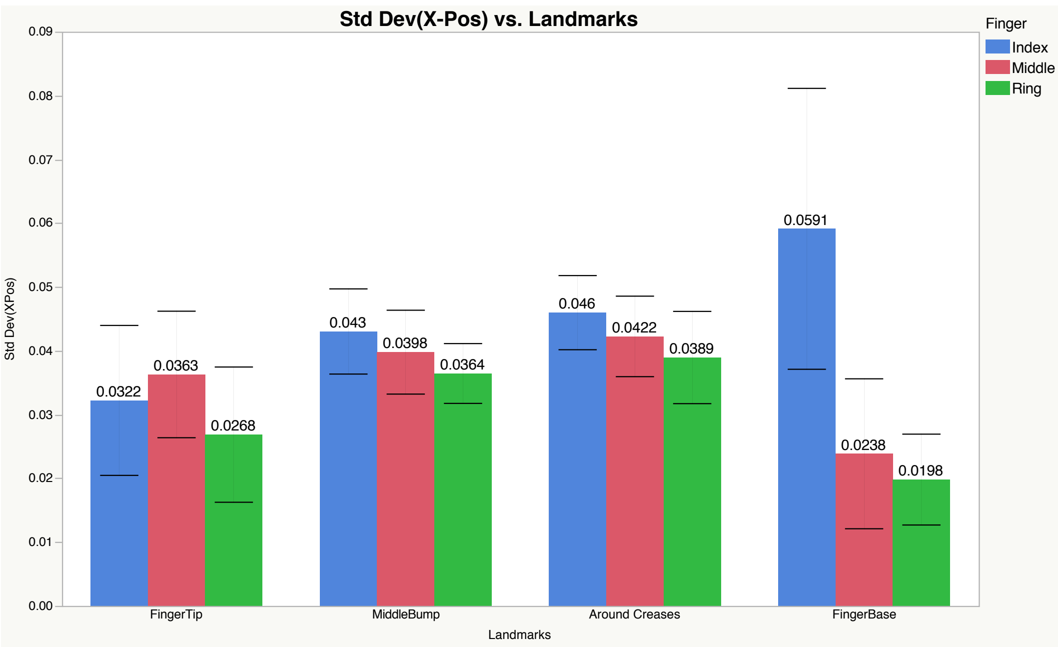

Figure 4.13: Landmark Analysis : Touch point spread for single row and double rows condition and Landmarks.

Single Row Condition

Furthermore, the spread is computed from the touch points per target, per finger, per participant for the single row condition alone. ANOVA (table 4.9) revealed no significant difference in the spread of touch points between targets or fingers in the single row condition. H2 was confirmed for the single row condition.

No significant differences in spread for the single row condition, H2 confirmed.

Source	DF	DFDen	F Ratio	Prob >F
Finger	2	78	0.1502	0.8607
Target	8	78	1.9398	0.0656
Finger*Target	16	78	1.2470	0.2533

Table 4.9: Spread Analysis : ANOVA with Bonferroni correction results of the spread of touch points, showed no significance.

Double Rows Condition

While for the double rows, ANOVA (table 4.10) revealed that the significant difference in the spread was due to the targets ($F_{3,105} = 1658.692, p < 0.0001$). While the finger and target condition had no main effect on the spread. This allowed us to confirm H3, and assume that the button size will be similar across the upper and lower row of the finger, and the 3 fingers. Furthermore, ANOVA (table 4.11) revealed that there is no significant difference in the spread across targets and fingers for normalised y-position for the upper and lower rows.

Targets had main effect on the spread, for the double rows condition.

Source	DF	DFDen	F Ratio	Prob >F
Finger	2	159	0.0931	0.9111
Target Condition	1	159	0.0499	0.8235
Finger*Target Condition	2	159	0.5149	0.5985
Target	8	159	3.6635	0.0006
Finger*TargetNUM	16	159	1.5458	0.0900
Target Condition*Target	8	159	0.8728	0.5408
Finger*Target Condition*Target	16	159	0.6715	0.8188

Table 4.10: Spread Analysis : ANOVA with Bonferroni correction results of the spread of touch points x-positions, 'targets' showed significants.

Furthermore, Tukey's post-hoc test showed that the significants in targets is due to targets 1 and 9 which are the

Source	DF	DFDen	F Ratio	Prob >F
Finger	2	159	0.1452	0.8649
Target	8	159	0.5701	0.8013
Finger*Target	16	159	2.1882	0.0074
Target Condition	1	159	2.3635	0.1262
Finger*Target Condition	2	159	0.7676	0.4658
TargetNUM*Target Condition	8	159	2.3164	0.0223
Finger*Target*Target Condition	16	159	1.0522	0.4057

Table 4.11: Spread Analysis : ANOVA with Bonferroni correction results of the spread of touch points y-positions, 'targets' showed significants.

Targets			Least Sq Mean
3	A		0.04410554
6	A		0.04389439
5	A	B	0.03777709
7	A	B	0.03699612
2	A	B	0.03506863
8	A	B	0.03368510
4	A	B	0.03288278
1		B	0.03041347
9		B	0.02873125

Table 4.12: Spread Analysis : Tukey's post-hoc test results for the touch point spread of the targets x-positions, for the double rows condition.

Significant effect is due to difference between targets near the tip and base, and between targets near creases.

smallest in spread, and targets 3 and 6 which are the largest in spread. Both targets 3 and 6 are located around the creases, as demonstrated in figure 4.2. It can be concluded that for the double row condition, targets before the crease were harder to locate.

In conclusion, it was deducted that the spread of touch points x-positions across fingers and targets will change, although change was not significant for the single row condition, in comparison to the double row condition. Furthermore, it was demonstrated that not all tactile cues on the finger have contributed to the accuracy of the touch points. Finally, there was no significant difference in the spread of touch points in y-position between targets, upper and lower rows and fingers.

Furthermore, we computed the button size we would overlay over the targets as follows :

To obtain the targets size (TS_x) for the X position data points in millimeters, we multiplied double the standard deviation by the average length of the finger.

Imaginary Button Size in x-direction:

$$TS_x = Average\ Finger\ Length * 2\sigma \quad (4.8)$$

Definition: *Imaginary Button Size in x-direction*

Furthermore, to obtain the targets size (TS_y) for the Y position data points in millimetres, we multiplied double the standard deviation by the average length between (YMaxValue - YMinValue) per finger.

Imaginary Button Size in y-direction:

$$TS_y = Mean(YMaxValue - YMinValue) * 2\sigma \quad (4.9)$$

Definition: *Imaginary Button Size in y-direction*

Previous results revealed that there was no significant difference in the spread across targets per finger, for the single row condition. Therefore, the average finger length for each of the index, middle and ring finger were measured, and the average button length in x and y were calculated, as demonstrated in tables 4.13 and 4.14.

Finger	Target Size X (mm)	Target Size Y (mm)	Avg. Finger length (mm)
Index	10.2	13.5	75.3
Middle	10.2	13.1	79.8
Ring	8.1	12.8	75.6

Table 4.13: Spread analysis : Average button size for single row condition per finger.

Furthermore, in tables A.1, A.2, A.3, A.4, A.5 and A.6 holds

Finger	Finger Condition	Target Size X (mm)	Target Size Y (mm)	Avg. Finger length (mm)
Index	Lower	8.8	3.6	75.3
Index	Upper	9.9	3.8	75.3
Middle	Lower	8.9	4.0	79.8
Middle	Upper	8.5	3.8	79.8
Ring	Lower	7.9	3.9	75.6
Ring	Upper	7.2	4.0	75.6

Table 4.14: Spread analysis : Average button size for double rows condition per finger.

the detailed finger size per target, for each finger.

4.12.3 Impact Angle Analysis

How does the orientation of thumb on finger change during the touching of the targets in both target conditions ? the impact angle allowed us to see to measure and compare the posture of the thumb over finger during touch of targets. The analysis of the impact angle can allow us to enhance the detection of certain targets, specially as some targets shows significant differences, that can distinguish them from other targets.

Target and finger had main effect on impact angle, and significant interaction effect between finger and target.

Single Row Condition
ANOVA with Bonferroni correction of the impact angle revealed that the target ($F_{8,821} = 119.1640, p < 0.0001$) had a significant effect on the impact angle. Furthermore, a significance in the interaction effect between the finger and target ($F(16, 821) = 6.9969, p < 0.0001$). While overall their was no significants in the angles across the fingers (table 4.15).

Impact angle can identify targets on different phalanges for the index and middle fingers.

Furthermore, Tukey's post-hoc test showed that targets on the same phalange had the same effect 1,2,4,6 and (8 or 9) on the index finger had different effect levels. Nevertheless,

Source	DF	DFDen	F Ratio	Prob >F
Target	8	821	119.1640	<.0001*
Finger	2	821	5.7216	0.0034
Target*Finger	16	821	6.9969	<.0001*

Table 4.15: Impact angle analysis : ANOVA with Bonferroni correction results for impact angle for the single row condition. 'Targets' showed significant effect on results, while interaction effect was also signficant.

for the middle finger, the number of identifiable targets decreases, as the effects of the target become more close. For the middle finger, only targets 1,2 and 4. Finally, for the ring finger, only target 1 (fingertip) was identifiable from the other targets.

Double Rows Condition

Moreover, it was revealed that the target ($F_{8,1649} = 237.3202, p < 0.0001$) and finger ($F_{2,1649} = 44.9381, p < 0.0001$) had a significant effect on the impact angle (table 4.16). Similar to the single row condition, a significance in the interaction effect between the finger and target ($F(16, 821) = 14.3919, p < 0.0001$). While overall their was no significants between the target conditions on the same fingers.

Target and finger had main effect on impact angle, and significant interaction effect between finger and target.

Source	DF	DFDen	F Ratio	Prob >F
Target Condition	1	1649	0.2183	0.6404
Target	8	1649	237.3202	<.0001
Finger	2	1649	44.9381	<.0001
Target Condition*Finger	2	1649	1.7713	0.1704
Target*Finger	16	1649	14.3919	<.0001
Target Condition*Target	8	1649	3.3588	0.0008
Target Condition*Target*Finger	16	1649	1.0822	0.3666

Table 4.16: Impact angle analysis : ANOVA with Bonferroni correction results for impact angle for the double rows condition. 'Targets' showed significant effect on results, while interaction effect was also significant.

Tukey's post-hoc test showed that targets on both conditions are similar in effect level, hence their was no distin-

No significant difference in the angles between upper and lower rows, while targets angles were significant between phalanges only.

guish between thumb on finger posture for both upper and lower targets. Furthermore, the angles in the double rows condition are not as distinct as the single row. The index finger had only 3 targets uniquely identified for each condition, one from each phalange (targets 1 or 2 or 3), (4 or 5 or 6) and (7 or 8 or 9). Moreover, middle finger post hoc test also exhibited only 3 identified targets per each condition, similar to the index finger configuration. While Finally for the ring finger there was no identifiable targets.

Post-hoc and measurement tables

Tables A.11, A.12, A.13 for the single row condition, while for the double row condition tables A.14 and A.15. We demonstrates the single row and double rows post-hoc tests tables, and the mean and standard deviation of the targets and angles with 95% confidence interval.

4.12.4 Implication

Target size of thumb on finger interaction showed similar size to other studies.

In comparison to the touch target size on the palm of the hand mentioned in chapter 2 “Related Work”, dfferent studies showed minimum button sizes of 15.0mm (Holz and Baudisch [2010]), 11.5mm (Wang and Ren [2009]) and 10.5mm (Vogel and Baudisch [2007]) for interacting on a touch screen. The touch distributions measured by Gustafson et al. [2011] on the palm of the hand indicated minimum button sizes of 9.5mm for their imaginary interface. Furthermore, subjects during our thumb interaction reached a similar targets size of average 10mm (single row condition) and 8mm (double rows condition) per target per finger.

creases are a vital mechanism for target localisation, not accuracy.

Furthermore, results showed no significants in spread between targets on the middle bump and targets on the creases, nevertheless, qualitative results showed that the creases were vital landmarks for locating the middle bump and near creases targets. Furthermore, using landmarks allowed a consistent layout across the fingers.

Timing showed around 2 seconds overall for touching and selection.

Furthermore, the selection time per touch was around 2 seconds in both conditions. The timing assume total blindness of the users interaction to their hands, hence this timing was due to the use of the landmarks as the guide for search. Nevertheless, the memory recall timing of the location of certain button such as the letters on keyboard in total blindness was not measured.

Furthermore, the impact angle had shown significance across targets on different phalanges. Moreover, it can be used for phalange selection before touch point projecting.

Impact angle used for phalange selection.

Chapter 5

Layout Evaluation

In this chapter, we evaluated the effectiveness of our 9 target conceptual layout in double and single row conditions. In the previous chapter, some targets spread and distance to neighbouring targets exhibited an overlaps with surrounding targets. we ought to evaluate how severe this overlapping will decrease our target effectiveness of touch and which targets will causes this degradation. Aiming to reach a layout that would allow a $> 90\%$ effectiveness of touch.

Searching for the optimal layout for imaginary keyboard layout.

Furthermore, the 9 targets conceptual layout could not reach the $> 90\%$ aim, we ought to evaluate all possible combinations of targets on the finger until we reach our goal. Our criteria of choosing the layout is finding the layout which holding the maximum number of touch targets while have an overall average layout effectiveness above 90%. Furthermore, this layout must hold this average effectiveness value across the 3 fingers.

5.1 Aim & Rationale

Evaluating the 9 target conceptual layout using the normalised touch points across all subjects.

In our evaluation of the conceptual layout and the alternative layouts, we used our normalised (x,y) positions mentioned in chapter 4 "User Study : The Conceptual Layout". Moreover, a distance-based classifier combined with

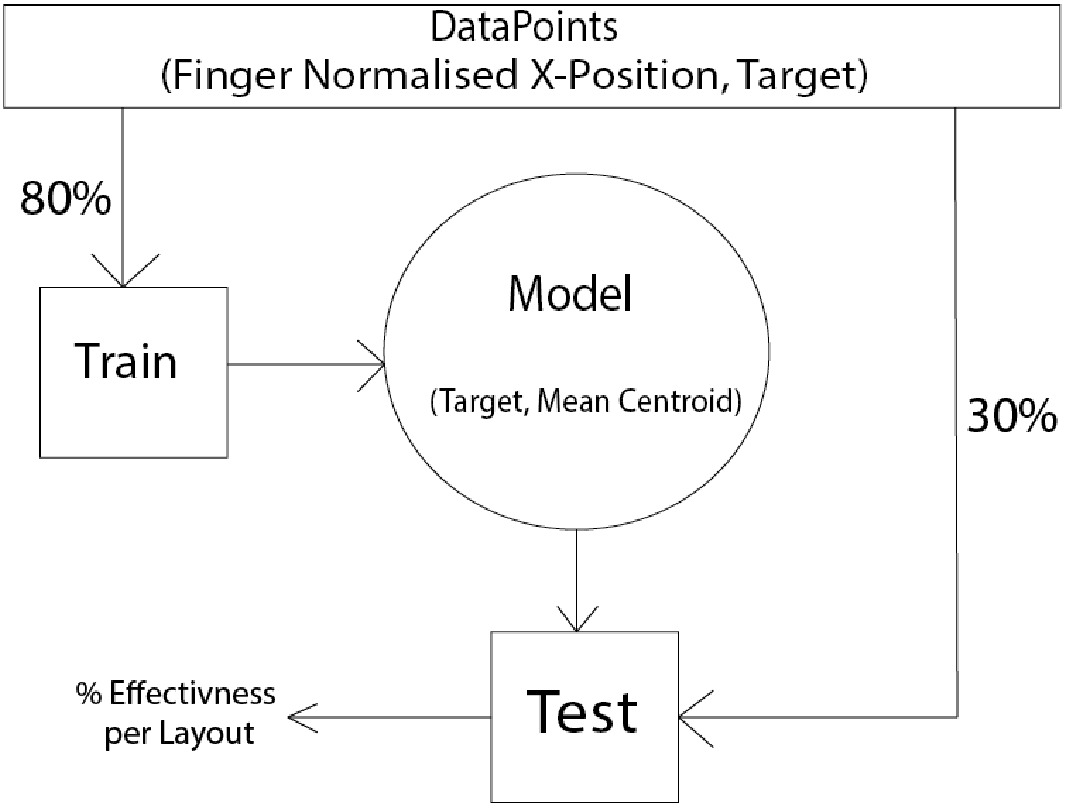

Figure 5.1: Evaluation : The testing and training procedure.

a 80/20 holdout cross validation method for partitioning the training and testing data, as demonstrated in figure 5.1.

Furthermore, to find the alternative layout, we generated all possible combinations of layouts with different number of targets per finger, and different combinations of targets per finger.

We investigated 7 classes of layouts, starting with simulating 3 targets per finger, up to the 8 targets per finger, and the same concept was used with the double rows condition. Each of these layout classes were evaluated for each of the 3 fingers, while all possible combinations of targets per each class layout were calculated.

Number of targets per layout starting from 3 up to 8 will change the effectiveness of targets.

For the double row condition, each of the classes were evaluated for the upper and lower side of the finger separately.

5.2 Independent Variables (IV)

1. *Three Fingers* - Index, Middle, Ring.

2. *Layout Class* - The classes of layouts varies from 3 to 9 Target per layout per Finger, each class with different target combination .

3. *Targets Conditions* - Single Row and Double Row

5.3 Dependent Variables (DV)

5.3.1 Target Effectiveness

The false negatives and false positives affect target effectiveness incase of target overlapping.

Furthermore, computing accuracy through only dividing the correct classifications by all classifications is not sufficient, specially for the intermedial and proximal phalange. For these two phalanges, the target width's are less than double their standard deviation. Thus, it will not be a fair assessment. Moreover, we believe that even if the targets covers all it's intended points, it can still overlap other targets, and decreasing their effectiveness.

Therefore, we added two more metrics precision and recall, which allowed us to compute the accuracy, while penalising the number of missed items by the classifier and the number of incorrect classifications, thus measuring the effectiveness of the target selection.

Definition: *Precision*

PRECISION:
The correct classifications penalised by the number of incorrect classifications.

$$\frac{true\ positives}{(true\ positives + false\ positives)} \tag{5.1}$$

RECALL:
The number of correct classifications penalised by the number of missed items.

$$\frac{true\ positives}{(true\ positives + false\ negatives)} \tag{5.2}$$

Definition: *Recall*

EFFECTIVENESS:
Derived from *F1 Measure* measurement. The resultant value is interpreted as a weighted average of the precision (5.1) and recall (5.2). The best value is 1 and the worst is 0.

$$\frac{2(precision * recall)}{(precision + recall))} \tag{5.3}$$

Definition: *Effectiveness*

5.4 Procedure & Configuration

5.4.1 Cross Validation

Due to the limited dataset obtained from our previous user study around 2407 point for our 4 participants, therefore due to our limited training and testing data, we applied a holdout cross validation method, partitioning the data into 80% training and 20% testing, with 10 repetitions from which our results were averaged among these repetitions.

80% of data used for training, 10% for testing, results are averaged over 10 repetitions in random.

5.4.2 Distance-Based Classifiers

Similar to the classification method carried by Findlater et al. [2011] in investigating typing on flat glass touch surfaces. In which the mean centroid of the key stroke and a distance based classifier were used for classifying the touch strokes for the different keyboard keys. we computed the mean centroids of our model using a 1-nearest neighbour classifier.

1-NN classifier is used for the classification method

Mean centroid per target is computed from the training data.

The mean centroid per each target was computed from the training data, and the euclidian distance was calculated between the testing data and the model mean centroid. Finally, each testing data point is classified according to the nearest first centroid neighbour to the touch point. In the single condition, the x-position only (5.4) was used in evaluation, while for the double rows condition the normalised x and y positions (5.5) were used.

$$D_x = \sqrt[2]{(Model_x - TestPoint_x)^2} \tag{5.4}$$

$$D_{x,y} = \sqrt[2]{(Model_x - TestPoint_x)^2 + (Model_y - TestPoint_y)^2} \tag{5.5}$$

5.4.3 Alternative Layout

466 different layouts generated as potential alternative to the original layout.

Attempting to find the alternative layout that will reach $> 90\%$, we generated 2^9 (512) different possible target layouts per each finger. We Disregarding the layouts that are below 3 targets per layout, allowing us to evaluate 466 different layouts. Layouts evaluation started from 3 targets per layout, in which only 3 targets were to be present on a finger, the effectiveness of all possible combinations are calculated. Furthermore, more alternative layouts up to 8 targets per layout, where we exclude only one target from the layout per each combination.

5.5 Statistical Methods

Similar to section 4.9 "Statistical Methods", ANOVA and post-hoc test were used to detect significants, effect levels and patterns. Nevertheless, the measure of effectiveness is used instead of the touch points and spread. In addition to a new independent variable which is the layout class.

5.6 Result Analysis

We extended the answer to our research questions from the previous chapter by measuring the effectiveness of the targets.

5.6.1 The 9 Target Conceptual Layout

Q1. What is the effectiveness of the targets given the 9 targets per finger layout, for the 3 fingers ? To answer this question, we used the methodology explained in section 5.4 "Procedure & Configuration" to measure the individual target effectiveness and the overall model effectiveness, for both single row and double rows conditions.

H1:
Targets at the tip(1) and base(9) of the finger will be highest in effectiveness.

Hypothesis:
H1

H2:
The index finger will have the least overall effectiveness, followed by the middle finger, and finally the ring finger as the most effective.

Hypothesis:
H2

Single Row Condition
ANOVA with Bonferroni correction (table 5.1), has revealed for the single row condition that the targets ($F_{(8,26)} = 3.1170$, $p < 0.0215$) has the main effect on the effectiveness of the 9 targets conceptual model, while the finger had no effect. Tukey post-hoc test (table 5.2) with each pair showed the target's main effect is due to target 1 (fingetip) and target's 5,7 and 8. While the other targets effect falls between these two sets. The overall 9 targets layout effectiveness on 3 fingers do not pass the $> 90\%$ effectiveness, which leads us to find an alternative layout.

Targets had the main effect on the effectiveness, this effect is due to target's 1,5,7 and 8.

Furthermore, figure 5.2 illustrates the leakage of touch

False negatives and false positives shown as lighter blue around targets aligned diagonally.

Source	DF	DFDen	F Ratio	Prob >F
Target	8	26	3.1170	0.0215*
Finger	2	26	1.3685	0.2736

Table 5.1: Effectiveness: ANOVA with Bonferroni results for effectiveness. 'Targets' showed significant effect on results, for single row condition.

Level				Mean
1	A			0.97118699
3	A	B		0.89110804
2	A	B		0.88514606
4	A	B	C	0.77430288
9	A	B	C	0.75954038
6		B	C	0.68163800
5			C	0.64868711
7			C	0.63486074
8			C	0.57540935

Table 5.2: Effectiveness : Tukey's post-hoc test results for effectiveness measurement . 'Targets' significant difference between target 1 and targets 5,7 and 8, for single row condition.

points on the surrounding targets per finger. The confusion matrix shows targets with higher effectiveness in dark red colours, and less effective ones are in more lighter blue shades, while dark blue colour is neutral. Targets classified correctly are along the diagonals, while targets false negatives and positives are in lighter blue colour near the diagonals. Overall, the figure shows more false positives around targets 5,6,7 and 8 along the 3 fingers this miss classification decreases. Furthermore, Figure 5.3, shows the percentage of effectiveness of the targets for the 3 fingers.

Hypothesis: *H4*

H4:
Targets on the upper side of the finger in the double row pattern will not differ in effectiveness from the lower side through all fingers.

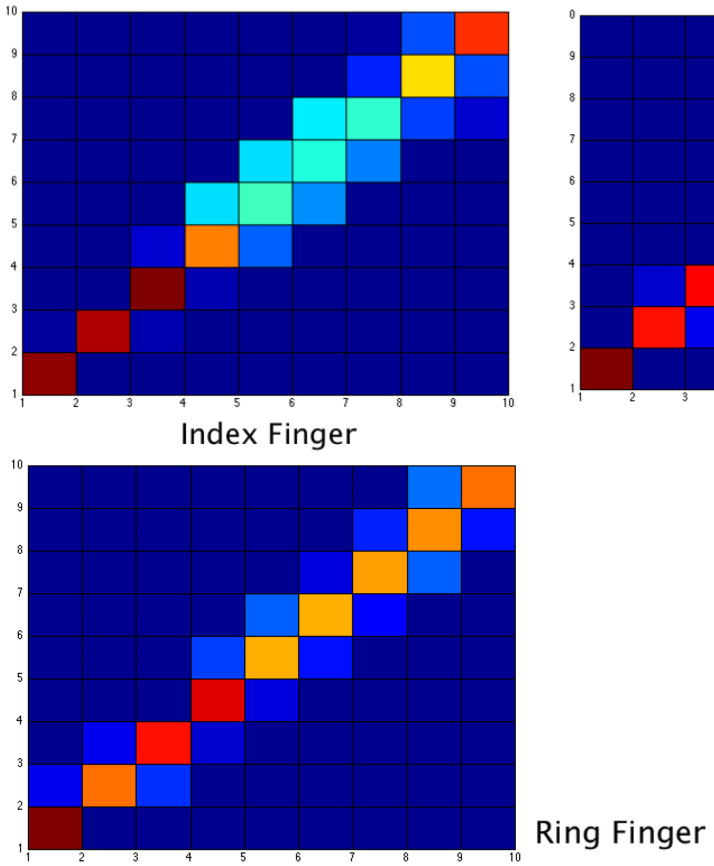

Figure 5.2: Effectiveness : Confusion matrix of targets classification for single row condition, higher effectiveness targets in dark red, while lighter blue is for lesser effectiveness. Dark blue is neutral.

Double Rows Condition

While for double rows condition, results has revealed that the targets ($F_{(8,53)} = 3.1170\,, p < 0.0001$) has the main effect on the effectiveness of the 9 targets conceptual model, while the upper or lower condition or finger had no effect on the layout effectiveness. there was also no significant difference in the interaction effect between fingers, conditions and target (table 5.3). Furthermore, post-hoc test showed that this significance was due to the difference in effect level between targets 1,3 and 2, and targets 5,7 and 8 (table 5.4).

Targets had the main effect on the layout effectiveness, effect is due difference between targets on distal and proximal phalange.

Similar to the confusion matrix figure aforementioned, figure 5.4 shows targets for the upper and lower rows on the 3 fingers. Furthermore, the percentage of false negative and

False negatives and positives is due to targets 5,6,7 and 8 in double rows condition.

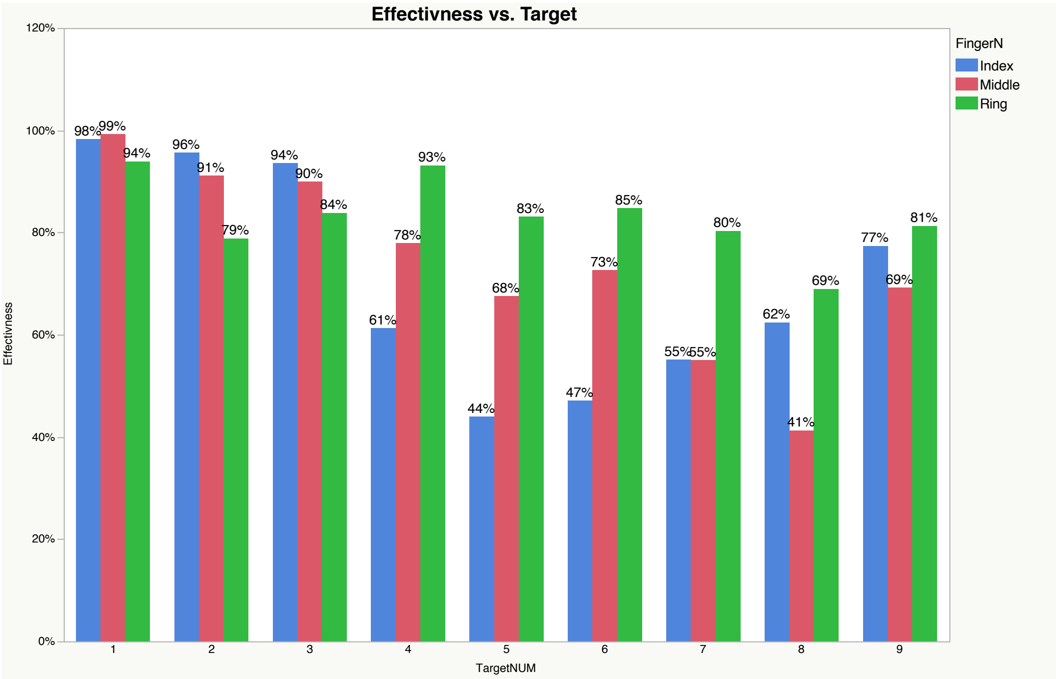

Figure 5.3: Effectiveness : Target effectiveness per target per finger, for single row condition.

positives in double rows for the targets on the inter medial and proximal phalange such as 5,6,7 and 8 are higher than the single row. Targets on the distal phalange are consistent in effectiveness across both target conditions. Figure 5.5, demonstrates the effectiveness of each target per finger per row.

5.6.2 Alternative Layouts

the 9 targets conceptual layout yielded $< 90\%$ effectiveness due to targets overlapping.

It was demonstrated that the 9 target conceptual layout yielded an effectiveness below 90%, due to overlapping effects of the adjacent targets specially on the intermedial and proximal phalange which led to many false negatives and false positives. Therefore, in this section we aimed to find a layout which can provide an above 90% effectiveness, while providing the maximum number of touch points possible.

Source	DF	DF Den	F Ratio	Prob >F
Target	8	53	14.9390	<.0001
Target Condition	1	53	0.1348	0.7184
Finger	2	53	0.5689	0.5772
Target Condition*Target	8	53	0.5547	0.7990
Finger*Target	16	53	0.6586	0.7937

Table 5.3: Effectiveness: ANOVA with Bonferroni results for effectiveness. 'Targets' showed significant effect on results, for single row condition.

Level						Least Sq Mean
1	A					0.87349303
3	A	B				0.79154108
2		B	C			0.68443202
4			C	D		0.59027611
6				D	E	0.49457626
9				D	E	0.47129270
7					E	0.39271467
5					E	0.38071607
8					E	0.35751784

Table 5.4: Effectiveness : Tukey's post-hoc test results for effectiveness measurement . 'Targets' significant difference between target 1 and targets 5,7 and 8, for the double row condition.

Q3. Which combination of targets (layout pattern) will have the highest effectiveness of selection per finger, given the number of targets required for an interaction ? As explained in section 5.1 "Aim & Rationale" and 5.4.3 "Alternative Layout", we have computed all possible combinations from 3 targets per layout up to 8 targets per layout, and computed the effectiveness of all layouts combination of targets to find the best layout.

Analyising the 466 different layouts using ANOVA with Bonferroni correction has revealed that the layout class $(F_{(6,62)} = 345.3114, p < 0.0001)$ had significant effect on the

Significant effect is due to layout class, finger and target condition.

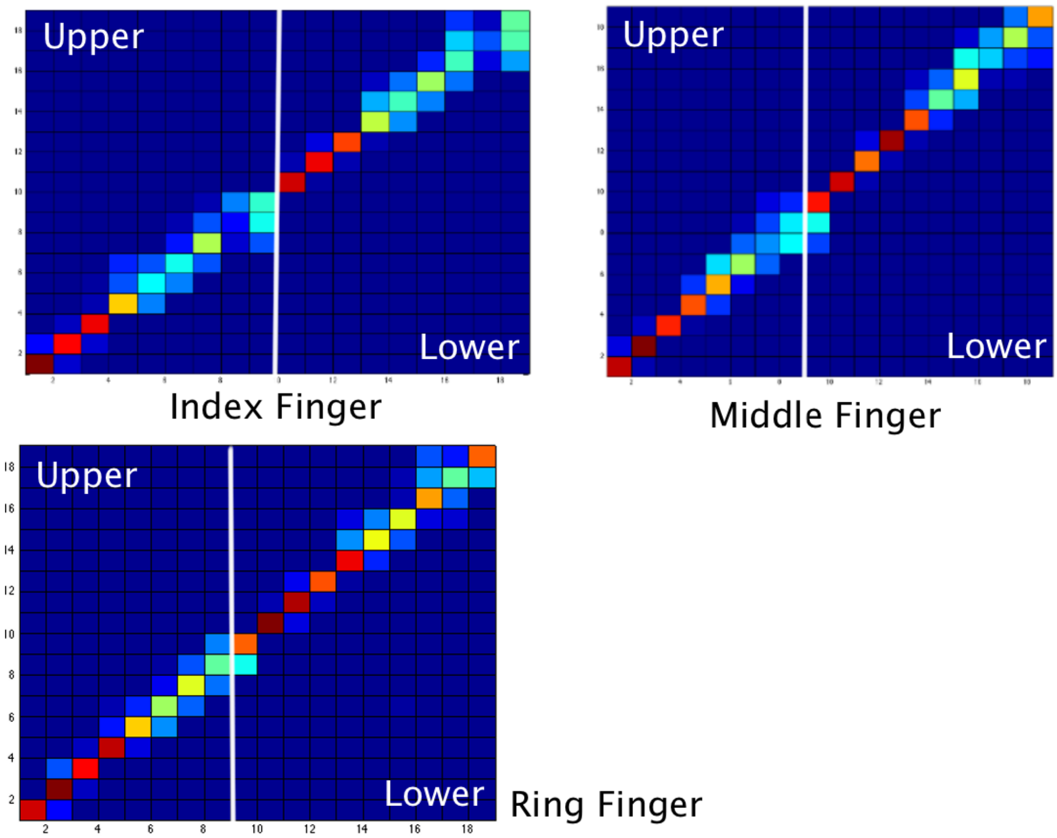

Figure 5.4: Effectiveness : Confusion matrix of targets classification for single row condition, higher effectiveness targets in dark red, while lighter blue is for lesser effectiveness. Dark blue is neutral.

effectiveness of the layouts as expected (table 5.5). Tukey post-hoc test showed that all layout classes between from 3 to 7 had different effect level while there was no significant effect between the 8 and 9 targets layout class (table 5.7).

no significant difference between upper and lower row on target effectiveness. Significant difference is due to single and double rows condition, while upper and lower rows had no significant difference.

Furthermore, the single row and doubles rows condition ($F_{(2,62)} = 47.4477$, $p < 0.0001$) also had a significant effect on the layout effectiveness, while there was no significant effect between the upper and lower rows for the double rows condition as shown in table 5.6.

Furthermore, a significant interaction effect with target number class and the target condition was found, while there was no effect of the finger on the effectiveness of the

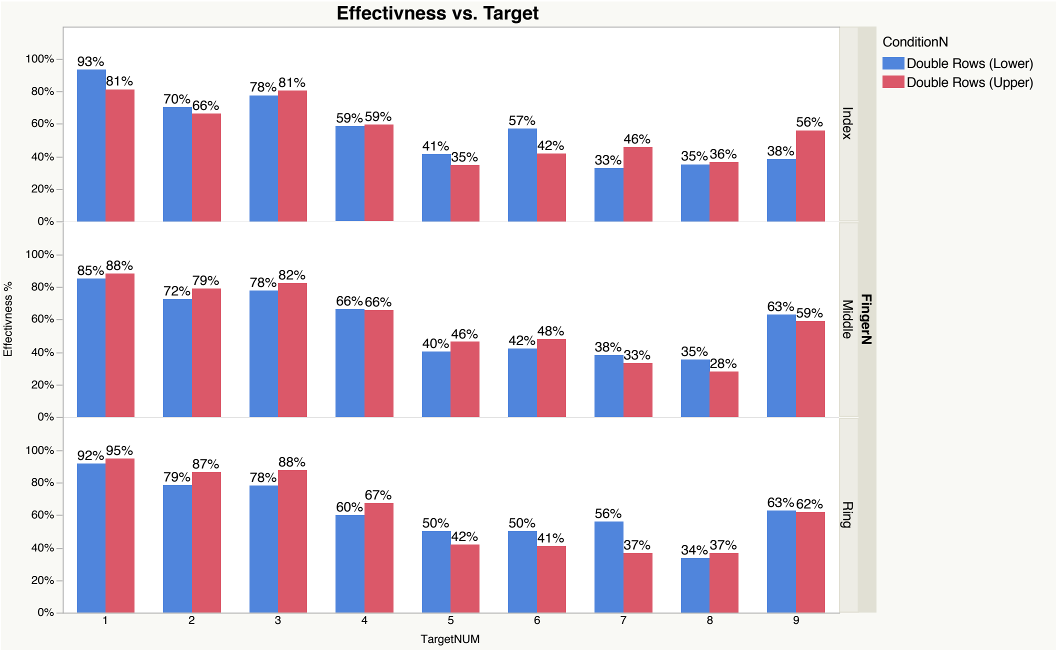

Figure 5.5: Effectiveness : Target effectiveness per target per condition per finger, for double row condition.

layouts.

The interpretation of these results lead us to believe that we may have more than one layout per target condition (Single row and double rows), nevertheless also the analysis revealed that the layout will be consistent over all fingers.

The final layout can be consistent over all fingers.

Single Row Condition

As shown in figure 5.6, as the number of targets per layout (layout class) decrease, effectiveness of the overall layout, with different target combination, increases. Furthermore, the 6 targets per layout class provided the $> 90\%$ effectiveness across 3 fingers, and attained the maximum number of targets per layout possible.

The 6 targets per layout for single row provide the best candidate as the alternative layout.

Source	DF	DFDen	F Ratio	Prob >F
Layout Class	6	62	345.3114	<.0001
Finger	2	62	7.5088	0.0005
Layout Class*Finger	12	62	1.6042	0.0828
Target Condition	2	62	47.4477	<.0001
Layout Class*Target Condition	12	62	7.5038	<.0001
Finger*Target Condition	4	62	0.1992	0.9389

Table 5.5: Effectiveness: ANOVA with Bonferroni results for effectiveness in alternative layouts. 'Class Layout', 'Target Condition' and 'Finger' showed significant effect on results, for single and double rows condition.

Level			Least Sq Mean
Single Row	A		0.92863711
Double Rows (Lower)		B	0.85608823
Double Rows (Upper)		B	0.85419910

Table 5.6: Effectiveness : Tukey's post-hoc test results for effectiveness measurement in alternative layouts. significance in target condition due to difference between single and double row.

Layout class							Least Sq Mean
3	A						0.87964148
4		B					0.83008251
5			C				0.78462457
6				D			0.74434753
7					E		0.70892390
8						F	0.67575916
9						F	0.64448170

Table 5.7: Effectiveness : Tukey's post-hoc test results for effectiveness measurement in alternative layouts. significance in layout class due to difference between layout classes 3 to 7.

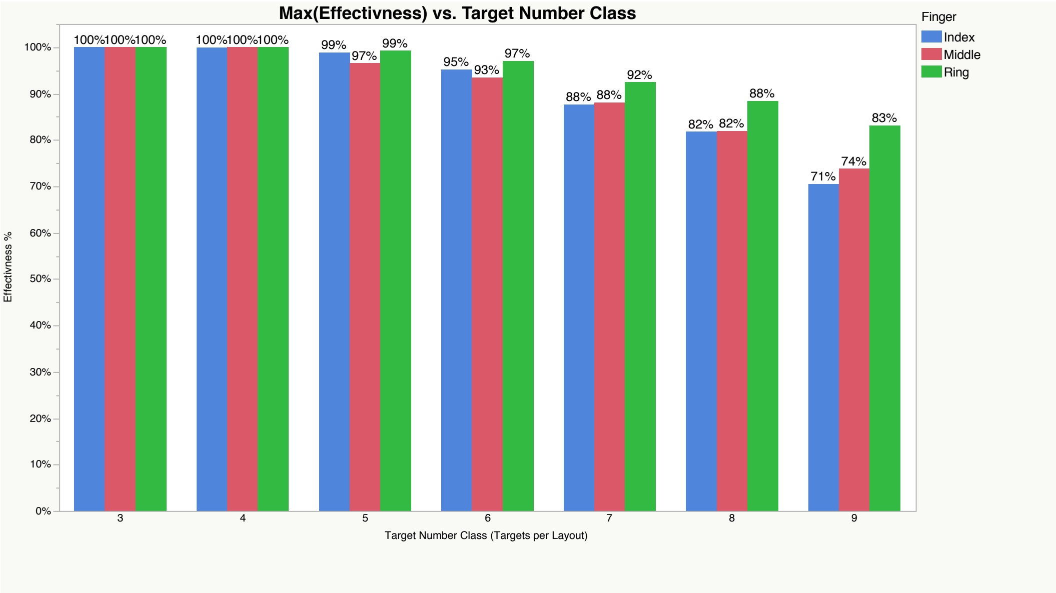

Figure 5.6: Effectiveness : Overall layout effectiveness per layout class, for single row condition.

Double Rows Condition

As shown in figure 5.7, the number of targets per layout decrease, effectiveness increases. Furthermore, the 4 targets per layout class provided the $> 90\%$ effectiveness across 3 fingers, and the double rows, and fulfilling the maximum number of targets per layout.

The 4 targets per layout for double rows provide the best candidate as the alternative layout.

Furthermore, tables 5.8 and 5.9 demonstrates all the targets patterns within the 6 and 8 targets layout which yields above $> 90\%$ effectiveness for the single row and double rows condition. the numbering in the *pattern* column is in the same ordered as demonstrated in figure 4.1 and 4.2.

5.7 Final Layout & Implication

In conclusion, our effectiveness measurements showed that the 9 targets conceptual layout did not reach our $> 90\%$ effectiveness criteria, as it was demonstrated for both single

one layout is chosen from the most effective layouts.

Pattern (Targets)	Index Finger	Middle Finger	Ring Finger
[1,2,3,4,6,9]	95.2%	93.5%	92.7%
[1,2,3,5,7,9]	94.1%	90%	92.6%
[1,2,3,4,7,9]	93.8%	90.3%	91.5%
[1,2,3,4,6,8]	92.6%	92.0%	92.6%

Table 5.8: Effectiveness : Top > 90% effectiveness layout for the single row condition, including the target combination pattern.

Figure 5.7: Effectiveness : Overall layout effectiveness per layout class, for double row condition.

Pattern	Index (Upper)	Index (Lower)	Middle (Upper)	Middle (Lower)	Ring (Upper)	Ring (Lower)
[1,3,5,8]	98.7%	96.9%	95.9%	95.8%	98.8%	98.1%
[1,3,4,8]	97.6%	97.8%	96.5%	96.5%	95.9%	96.0%
[1,3,4,9]	97.4%	98.4%	97.1%	96.5%	97.1%	98.8%
[1,2,4,8]	96.9%	93.1%	93.0%	94.4%	95.2%	97.7%
[1,3,6,8]	96.5%	94.2%	90.3%	92.2%	93.6%	96.7%
[1,3,4,7]	96.3%	96.5%	97.1%	94.1%	97.7%	98.4%
[1,2,4,9]	95.1%	91.1%	92.1%	95.5%	95.6%	96.8%
[1,3,6,9]	94.8%	97.8%	96.1%	98.3%	97.6%	98.4%
[1,2,4,7]	93.8%	90.8%	93.7%	92.3%	94.6%	97.0%
[1,3,5,7]	93.3%	93.0%	93.7%	91.8%	97.9%	94.7%

Table 5.9: Effectiveness : Top $> 90\%$ effectiveness layout for the double rows condition, including the target combination pattern.

row and the double rows condition. hence,an alternative layouts was needed.

After running the procedure aforementioned in section 5.4 “Procedure & Configuration”, we deduced the layouts as demonstrated in table 5.8 and 5.9. These targets had shown a consistency across all 3 fingers, and for the double row condition, on the upper and lower rows. Furthermore, we have chosen one layout from each of these combinations using data from our previous qualitative and quantitative analysis in chapter 4 “User Study : The Conceptual Layout”.

Single Row Condition

For the single row condition, the pattern [1,2,3,4,6,9] shown in figure 5.8, was chosen to be our recommended pattern. First, the targets overlay the 3 targets on the distal phalange, 2 on the intermedial phalange and one on the proximal phalange.

Targets were chosen near the creases, and on the distal phalange.

In this layout, only the creases targets were chosen for the intermedial phalange (targets 4 and 6), while all the distal phalange were chosen as they provide to be most effectiveness. Finally, in our qualitative analysis, it was shown that targets on the proximal phalange were the worst, while

Quantitative and qualitative analysis concluded that touch on the proximal phalange should be minimal.

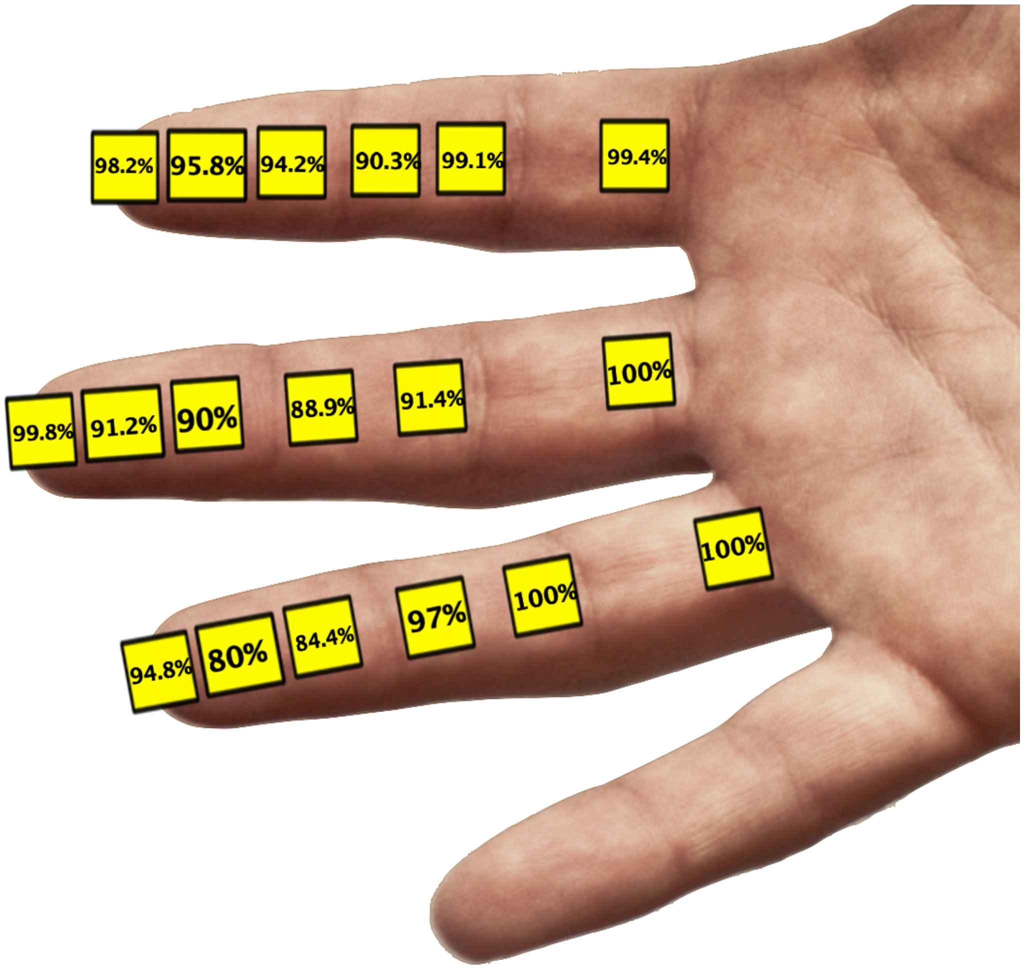

Figure 5.8: .
]Final layout : 6 targets per finger layout for the 3 fingers and single row condition. the pattern of targets [1,2,3,4,6,9].

middle bump targets were ambiguous to select. Therefore, middle bumps on the intermedial and proximal phalange were omitted, while for the proximal phalange had only one target located at the base to be easy and fast to find. Overall, this layout also have shown consistency in effectiveness across fingers and targets.

Double Rows Condition

Effectivness of targets on the upper and lower rows were consistent.

For the double rows condition, the pattern [1,3,4,7] shown in figure 5.8, was chosen to be our recommended pattern.

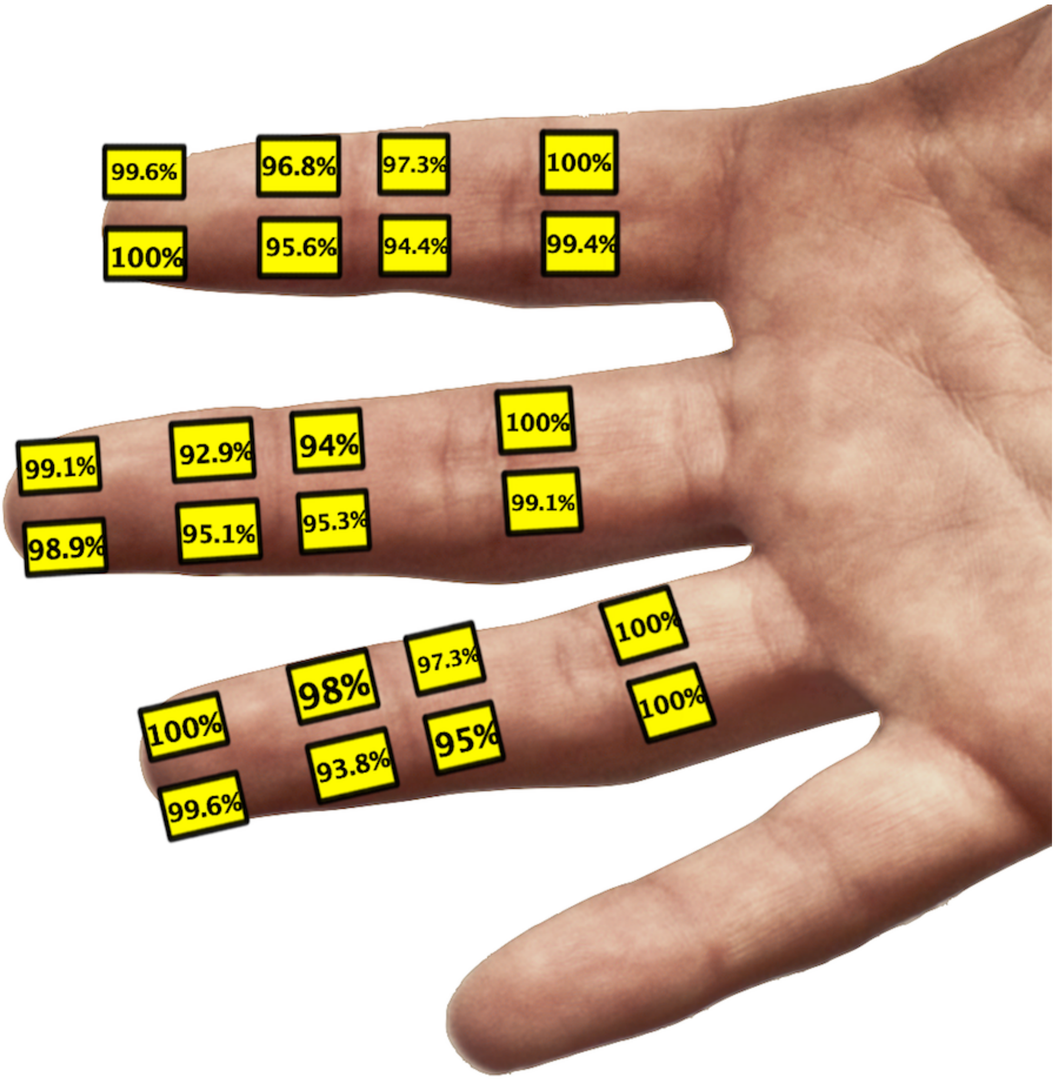

Figure 5.9: .
]Final layout : 8 targets per finger layout for the 3 fingers and double rows condition. the pattern of targets [1,3,4,7].

First, the layout overlay 2 targets on the distal phalange, 1 on the intermedial phalange and 1 on the proximal phalange. Furthermore, layouts that have more than one targets on the proximal phalange were avoided.The layout was used for both the upper and lower row, for consistency. All targets exhibited an $> 90\%$ effectiveness measurement for both rows.

5.8 Limitations

The limitation of our ability to generalise these layouts and our previous analysis, was due to the following :

Follow-up Study

The final layouts were not tested through a user study, but a simulated touch analysis.

Another limitation is the lack of a follow-up study that would validate our layouts, as the points tested for these layouts are computed from the previous 9 targets conceptual model and the use of the cross validation to randomise the points. Nevertheless, while these layouts provide an $> 90\%$ effectiveness, the percentage may vary with a real user interaction.

Hand Size & Finger Length

Different hands have different sizes, e.g. sizes are classified using standard glove measurement.

Although one of the benefits of using the bare hand technique over the glove based system for interaction, is that no adjustments needed or fitting to the hand. Moreover, the target touch points tested were relative to the landmarks aforementioned which are theoretically in a similar ratio along different hand sizes, nevertheless, the hand sizes is threaten the external validity of our study. we did not experiment with a variety of hand sizes, which limit our findings to a certain size. This size can be classified as small/medium based on the glove measurement system. (Havas).

Gender and Age

Index to ring finger ratio differs with age and gender.

It was demonstrated by Gillam et al. [2008] that gender and age had a main effect on the index and ring finger ratio, also known by the 2D 4D ratio and length. as it was shown that their a strong correlation between the increases in 2D:4D ratio as age increases.

Hand width and length varies between female and male.

Furthermore, Agnihotri et al. [2005] examined two hundred and fifty students (125 males and 125 females) of the age above 18 years in the year 2005, their study showed that the mean and standard deviation of the hand length and breadth changes across gender. In their study, male subjects have exhibited an increase of the hand length and breadth (width) over female subjects for both left and right hands.

Chapter 6

Summary and future work

During this thesis, we investigated different aspects of the finger and thumb interaction. Current on-body interactions and technologies have been reviewed and various aspects of the thumb on finger technique, such as to the precision, effectiveness and quality of the interaction were analysed. Guidelines and different layouts for the imaginary interface was designed and evaluated. This chapter summarises the work done throughout this thesis and demonstrates possible future work which could enhance the results and user interaction.

6.1 Summary and contributions

Recent wearables lacks a discreet text input mechanism.

Chapter 1 highlighted the lack of text input on recent wearable on-body devices and how it limits user's experience and usage of the devices. Moreover, it was argued that the use of voice recognition and microphones such as in dictation applications as an alternative can be inconvenient due to surrounding noise or the sensitivity of the content being dictated.

Wearables such as gloves for texting conceals hand tactile cue and could hinder movement.

Furthermore, new technologies emerged which utilises the hands for interaction, such as wearable gloves for texting, Nevertheless, they could become intrusive, while also it was proved that the tactile cues of the hand and fingers can allow a useable eyes-free interaction.

In our related work review (Chapter 2), we discovered many commercial technologies utilising the thumb on finger interaction, while we found no user oriented studies which focuses on the interaction using the thumb over fingers. Nevertheless, we reviewed studies that investigate on-body eyes-free interaction, utilising the finger touch over palm, or other body parts such as the ears as an input device. Measuring the interaction precision, timing for interaction and hand postures and patterns in interaction. We ought to measure same variables for the thumb on finger.

no user oriented study on the thumb over finger interaction, despite it's use in commercial products.

Moreover, the thumb over finger interaction was built into 4 main pillars, which are movements and articulations, affordance of the fingers shape, proprioceptive abilities and tactile landmarks (Chapter 3). these pillars were used in the development of the keyboard imaginary button layout guideline over the fingers using the thumb.

The imaginary keyboard is built on hand articulation, hand shape & affordance, proprioception and tactile landmarks.

The finger articulations and movements lead to defining tracking points of the hand articulation points on the finger and thumb joints and metacarpal bones of the palms, while determining the phalange on which the thumb touch will be projected.

Finger articulation used for tracking.

Tactile landmarks of the finger were classified into 3 categories, fingertip and finger base which is located at the end of the finger and on the boarder of the palm. Creases and skin folds near the joints and finger articulations, and the middle bumps located on the pulp flesh between each two landmarks e.g. tip and crease on the distal phalange, crease and crease on the intermedial phalange.

Creases and skin folds, fingertip and ends, and pulp flesh on phalanges used as guides.

Furthermore, the shape of the finger showed the affordance for touching along it's width in multiple areas. Furthermore, we mainly focused on the extreme ends along the curved width of finger. This allowed us to compute the quality and behaviour of touch across different areas of the

Finger curvature give the affordance of multiple touch along the finger width.

finger using the thumb.

The 9 targets Conceptual layout form the bases of our imaginary touch keyboard on the hand.

In our user study (Chapter 4), touch points were placed around the finger landmarks to create a conceptual layout forming the bases of our keyboard in an eyes-free interaction. The precision and time needed for selection of targets for this conceptual layout is measured. Targets were placed on the the tip and base of the fingers, on the middle bump of each phalange, and around the crease separating each finger, yielding a 9 targets per finger layout (single row condition), with a configuration of 3 targets per phalange on each finger. Furthermore, the same layout was extended on to both curved ends along the finger width, yielding 6 targets per each phalange, and a total of 16 targets per finger layout (double rows condition).

The 16 targets Conceptual layout is an alternative utilising the finger curvature.

Hand motion was classified into two hand postures used for touching.

Participants were not guided to how they should touch these targets using their thumb. Furthermore, qualitative analysis showed that during the sessions two postures for the thumb and finger interaction emerged. The first posture was the thumb touching the finger, in which the fingers become a ridged plane and the thumb moves to touch over the fingers, while for the other posture, the fingers moved to touch the thumb. In the latter posture, the finger articulates and moves until it reaches the thumb or both the thumb and fingers reach half ways. The earlier interaction was only seen once during the session, while most subjects used the fingers to touch the thumb, the posture can affect the tracking technique of the interaction.

Qualitiative analysis showed discomfort around the centre of palm in excessive use among male participants only.

Furthermore, targets on the proximal phalange near the base of the finger were also perceived by participants as inconvenient, and caused cramps around the Flexor digiti minimi brevis and Palmaris Longus muscles of the palm of the hand with excessive use among male participants only. While the middle bumps targets were stated to be the hardest to locate.

The tip and base of the fingers were easiest to find and select, while middle bump was the hardest.

Time taken for the selection of targets have revealed to be 1.8 - 2.7 seconds per target. While targets at the tip and base of the finger measured the fastest yielding 1.8 seconds, there was no significant difference in timing across fingers or conditions (single row and double rows). the slow timing of the middle bump and creases on the intermedial and proximal phalange were due to the multiple alternating of the participants thumb between each two landmarks surrounding the the target.

The spread of the targets was measured, by computing double the standard deviation of each of the targets touch points along the finger. The results had shown that the targets on the tip and base of the finger was the most accurate. Nevertheless, the spread of the same targets had no significant effect across different fingers.

The spread between the fingertip and base revealed to be the most accurate landmarks.

Furthermore, results also showed the touch button size of the imaginary keyboard which was 10mm (single row condition) and 8mm (double row condition). Using the landmarks allowed to overlay a keyboard of 10mm per key which is the size of a standard touch keyboard of a touch screen phone in landscape mode.

Using the landmarks and thumb interaction we can operate an imaginary keyboard of 10mm touch key size.

In our evaluation(Chapter 5), we used a distance-based classifiers, while partitioning data using cross validation into testing and training data, we measured 265 possible combinations of targets per layouts. We aimed to find the best layout which achieved a $> 90\%$ effectiveness while attaining the maximum number of targets per finger. it was revealed that best layout is 6 targets per finger (single row condition) or 8 targets per finger, 4 on the upper and lower row per finger (double rows condition).

The original 9 and 16 target conceptual target was replaced by the 6 and 8 targets per layout for increasing effectiveness.

It was concluded that a QWERTY keyboard will require two hands interaction, with a of maximum 6 or 8 targets on each finger. This is similar to holding the keyboard in landscape mode.

Finally, the impact angle, the angle of touch between the intersection of the thumb direction and the finger direction had demonstrated a significants across targets, fingers and target conditions. the significants difference was due to targets across different phalanges, on the other hand, targets of the same phalange were not significantly different. Impact angle can be used to detect the phalange by which the thumb touch will be projected on.

Impact angle can be used to detect which phalange the thumb touch point will be projected on.

6.2 Future work

Age, gender and hand size limitations used as independent variables.

- In chapter 5.8 “Limitations”, we mentioned limitations that have faced this thesis, such as the effect of the difference in age and gender on the finger ratios, and difference in hand sizes. Further studies need to be conducted using these limitations as research variables to conclude if our derived layouts will be consistent across these variation, for if change will be made.

The memory recall time measure for symbolic link of finger landmarks and keyboard letters.

- The landmarks showed that we can overlay an imaginary touch keyboard of 10mm width per key. Furthermore, we need to measure the transfer learning and memory recall time, similar to the study by Gustafson et al. [2011], to measure users ability to symbolically link the keyboard touch keys letters to the finger landmarks tactile and proprioceptive sense aforementioned using our concluded layout.

Using the computed layouts with new sensory technologies.

- In chapter 2 “Related Work” we discussed in the implementation section, new technologies such as FIN (RHLVisionTechnologies [2014]) and MYO (ThalmicLabs [2013]) which are non vision based tracking systems of the thumb and fingers. These technologies can use our user layouts as guidelines to test the effectiveness of these layouts against these technologies, to get closer to a more mobile solution for texting.

Appendix A

Lists & Tables

Finger	Target	SDx	SDy	Finger Length (mm)	Target Size X (mm)	Target Size Y (mm)
Index	1	0.03	0.16	75.28	4.31	6.56
Index	2	0.04	0.13	75.30	6.75	5.36
Index	3	0.04	0.15	75.30	6.15	6.00
Index	4	0.06	0.17	75.30	8.32	6.98
Index	5	0.05	0.16	75.30	7.66	6.27
Index	6	0.06	0.17	75.29	9.30	6.74
Index	7	0.07	0.15	75.30	10.35	5.93
Index	8	0.05	0.19	75.29	7.09	7.65
Index	9	0.05	0.21	75.30	7.20	8.35

Table A.1: Spread analysis : Index finger imaginary button size for single row conditions.

Finger	Target	SDx	SDy	Finger Length (mm)	Target Size X (mm)	Target Size Y (mm)
Middle	1	0.03	0.13	79.80	5.27	5.15
Middle	2	0.04	0.10	79.89	6.29	3.97
Middle	3	0.05	0.11	79.78	8.30	4.21
Middle	4	0.07	0.12	79.85	11.69	4.96
Middle	5	0.08	0.12	79.80	13.41	4.99
Middle	6	0.04	0.12	79.73	6.49	4.91
Middle	7	0.05	0.12	79.85	8.31	4.64
Middle	8	0.05	0.13	79.72	8.55	5.09
Middle	9	0.07	0.13	79.80	10.49	5.29

Table A.2: Spread analysis : Middle finger imaginary button size for single row conditions.

Finger	Target	SDx	SDy	Finger Length (mm)	Target Size X (mm)	Target Size Y (mm)
Ring	1	0.03	0.13	75.63	4.83	5.01
Ring	2	0.06	0.15	75.63	8.84	6.13
Ring	3	0.06	0.17	75.63	9.51	6.61
Ring	4	0.03	0.10	75.55	4.45	3.86
Ring	5	0.03	0.11	75.63	4.92	4.32
Ring	6	0.04	0.08	75.63	5.50	3.35
Ring	7	0.04	0.13	75.63	5.39	5.10
Ring	8	0.03	0.10	75.63	5.00	4.15
Ring	9	0.05	0.08	75.76	7.24	3.20

Table A.3: Spread analysis : Ring finger imaginary button size for single row conditions.

Finger	Target Condition	Target	SDx	SDy	Finger Length	Target Size X (mm)	
Index	Lower	1	0.04	0.07	75.30	5.48	2.91
Index	Lower	2	0.04	0.09	75.30	6.19	3.56
Index	Lower	3	0.07	0.08	75.30	9.97	3.16
Index	Lower	4	0.04	0.08	75.30	5.84	3.11
Index	Lower	5	0.05	0.09	75.30	7.62	3.79
Index	Lower	6	0.06	0.06	75.33	9.34	2.49
Index	Lower	7	0.09	0.10	75.30	13.44	4.1
Index	Lower	8	0.07	0.09	75.30	9.86	3.74
Index	Lower	9	0.07	0.14	75.30	11.25	5.57
Index	Upper	1	0.06	0.11	75.30	8.98	4.22
Index	Upper	2	0.05	0.13	75.30	7.32	5.03
Index	Upper	3	0.05	0.10	75.29	8.12	4.02
Index	Upper	4	0.05	0.12	75.30	6.79	4.60
Index	Upper	5	0.06	0.10	75.30	9.44	3.92
Index	Upper	6	0.08	0.11	75.30	11.99	4.34
Index	Upper	7	0.08	0.07	75.32	12.37	2.91
Index	Upper	8	0.08	0.08	75.30	12.15	3.02
Index	Upper	9	0.09	0.07	75.28	12.81	2.89

Table A.4: Spread analysis : Index finger imaginary button size for double rows conditions.

Finger	Target Condition	Target	SDx	SDy	Finger Length	Target Size X (mm)	
Index	Lower	1	0.04	0.07	75.30	5.48	2.91
Index	Lower	2	0.04	0.09	75.30	6.19	3.56
Index	Lower	3	0.07	0.08	75.30	9.97	3.16
Index	Lower	4	0.04	0.08	75.30	5.84	3.11
Index	Lower	5	0.05	0.09	75.30	7.62	3.79
Index	Lower	6	0.06	0.06	75.33	9.34	2.49
Index	Lower	7	0.09	0.10	75.30	13.44	4.1
Index	Lower	8	0.07	0.09	75.30	9.86	3.74
Index	Lower	9	0.07	0.14	75.30	11.25	5.57
Index	Upper	1	0.06	0.11	75.30	8.98	4.22
Index	Upper	2	0.05	0.13	75.30	7.32	5.03
Index	Upper	3	0.05	0.10	75.29	8.12	4.02
Index	Upper	4	0.05	0.12	75.30	6.79	4.60
Index	Upper	5	0.06	0.10	75.30	9.44	3.92
Index	Upper	6	0.08	0.11	75.30	11.99	4.34
Index	Upper	7	0.08	0.07	75.32	12.37	2.91
Index	Upper	8	0.08	0.08	75.30	12.15	3.02
Index	Upper	9	0.09	0.07	75.28	12.81	2.89

Table A.5: Spread analysis : Middle finger imaginary button size for double rows conditions.

Finger	Target Condition	Target	SDx	SDy	Finger Length	Target Size X (mm)	
Index	Lower	1	0.04	0.07	75.30	5.48	2.91
Index	Lower	2	0.04	0.09	75.30	6.19	3.56
Index	Lower	3	0.07	0.08	75.30	9.97	3.16
Index	Lower	4	0.04	0.08	75.30	5.84	3.11
Index	Lower	5	0.05	0.09	75.30	7.62	3.79
Index	Lower	6	0.06	0.06	75.33	9.34	2.49
Index	Lower	7	0.09	0.10	75.30	13.44	4.1
Index	Lower	8	0.07	0.09	75.30	9.86	3.74
Index	Lower	9	0.07	0.14	75.30	11.25	5.57
Index	Upper	1	0.06	0.11	75.30	8.98	4.22
Index	Upper	2	0.05	0.13	75.30	7.32	5.03
Index	Upper	3	0.05	0.10	75.29	8.12	4.02
Index	Upper	4	0.05	0.12	75.30	6.79	4.60
Index	Upper	5	0.06	0.10	75.30	9.44	3.92
Index	Upper	6	0.08	0.11	75.30	11.99	4.34
Index	Upper	7	0.08	0.07	75.32	12.37	2.91
Index	Upper	8	0.08	0.08	75.30	12.15	3.02
Index	Upper	9	0.09	0.07	75.28	12.81	2.89

Table A.6: Spread analysis : Ring finger imaginary button size for double rows conditions.

Targets	Finger													Least Sq Mean
1	Index												L	-0.1363385
2	Index										J			0.0437969
3	Index								H					0.1851669
4	Index							G						0.3715161
5	Index						F							0.4464850
6	Index					E								0.5347608
7	Index				D									0.6398970
8	Index		B	C										0.7388290
9	Index	A												0.8193389
1	Middle												L	-0.1394451
2	Middle										J	K		0.0241726
3	Middle								H	I				0.1552280
4	Middle							G						0.3625823
5	Middle						F							0.4454233
6	Middle					E								0.5029599
7	Middle				D									0.6310700
8	Middle			C										0.6994654
9	Middle	A	B											0.7784833
1	Ring												L	-0.1821764
2	Ring											K		-0.0122018
3	Ring									I				0.1333070
4	Ring							G						0.3387131
5	Ring						F							0.4295576
6	Ring					E								0.5147381
7	Ring				D									0.6388967
8	Ring			C										0.7091801
9	Ring	A												0.7877642

Table A.7: Touch point analysis : Post-Hoc test for the touch point x-positions, for the 3 fingers and single row condition.

Target	Condition	Finger																								
1	Lower	Index																					V	W	X
2	Lower	Index																			T	U			
3	Lower	Index																		S					
4	Lower	Index															P	Q							
5	Lower	Index												M	N	O	P								
6	Lower	Index										K	L												
7	Lower	Index							G	H															
8	Lower	Index					E	F	G																
9	Lower	Index		B	C	D	E																		
1	Upper	Index																					V		
2	Upper	Index																			T				
3	Upper	Index																	R						
4	Upper	Index												M	N	O									
5	Upper	Index										J	K	L											
6	Upper	Index									I	J													
7	Upper	Index					E	F	G																
8	Upper	Index		B																					
9	Upper	Index	A																						

Table A.8: Touch point analysis : Post-Hoc test for the touch point x-positions, for the index finger and double rows condition.

Target	Condition	Finger																							
1	Lower	Middle																						W	X
2	Lower	Middle																		T	U				
3	Lower	Middle																	S						
4	Lower	Middle															Q								
5	Lower	Middle											M	N											
6	Lower	Middle								J	K	L													
7	Lower	Middle						H																	
8	Lower	Middle				F	G	H																	
9	Lower	Middle	B	C	D	E																			
1	Upper	Middle																				V	W		
2	Upper	Middle																		T	U				
3	Upper	Middle																R	S						
4	Upper	Middle												N	O	P	Q								
5	Upper	Middle										L	M												
6	Upper	Middle							I																
7	Upper	Middle				F	G	H																	
8	Upper	Middle		C	D	E	F																		
9	Upper	Middle	B	C																					

Table A.9: Touch point analysis : Post-Hoc test for the touch point x-positions, for the middle finger and double rows condition.

Target	Condition	Finger																				
1	Lower	Ring																				X
2	Lower	Ring																			U	
3	Lower	Ring																	S			
4	Lower	Ring															Q					
5	Lower	Ring											M	N								
6	Lower	Ring							I	J	K	L										
7	Lower	Ring						H														
8	Lower	Ring				E	F															
9	Lower	Ring	B	C	D	E																
1	Upper	Ring																				X
2	Upper	Ring																		T	U	
3	Upper	Ring																R	S			
4	Upper	Ring													O	P	Q					
5	Upper	Ring										L	M									
6	Upper	Ring							I	J	K											
7	Upper	Ring						H														
8	Upper	Ring			D	E	F															
9	Upper	Ring	B	C	D																	

Table A.10: Touch point analysis : Post-Hoc test for the touch point x-positions, for the ring finger and double rows condition.

Target	Finger	Condition	N Rows	Mean	Std. Dev	Upper 95% CI	Lower 95% CI
1	Index	Single Row	31	89.76	11.26	93.72	85.79
2	Index	Single Row	32	73.56	13.36	78.19	68.93
3	Index	Single Row	32	65.52	16.39	71.19	59.84
4	Index	Single Row	32	54.06	12.07	58.24	49.88
5	Index	Single Row	32	52.59	10.95	56.38	48.80
6	Index	Single Row	31	50.34	12.56	54.76	45.92
7	Index	Single Row	32	43.14	4.19	44.59	41.69
8	Index	Single Row	31	37.75	7.41	40.36	35.14
9	Index	Single Row	32	38.49	8.31	41.37	35.62

Table A.11: Impact angle Analysis : Index finger single row conditions, mean, standard deviation and 95% confidence interval.

Target	Finger	Condition	N Rows	Mean	Std. Dev	Upper 95% CI	Lower 95% CI
1	Middle	Single Row	32	94.68	13.75	99.44	89.92
2	Middle	Single Row	31	78.05	13.36	82.76	73.35
3	Middle	Single Row	30	74.12	12.02	78.42	69.82
4	Middle	Single Row	31	63.10	9.00	66.26	59.93
5	Middle	Single Row	32	66.60	10.60	70.27	62.93
6	Middle	Single Row	31	65.41	6.70	67.76	63.05
7	Middle	Single Row	31	58.35	8.08	61.20	55.51
8	Middle	Single Row	31	58.02	10.83	61.83	54.21
9	Middle	Single Row	32	55.29	9.95	58.74	51.84

Table A.12: Impact angle Analysis : Middle finger single row conditions, mean, standard deviation and 95% confidence interval.

Target	Finger	Condition	N Rows	Mean	Std. Dev	Upper 95% CI	Lower 95% CI
1	Ring	Single Row	32	99.29	22.61	107.12	91.45
2	Ring	Single Row	32	87.26	14.04	92.12	82.39
3	Ring	Single Row	32	83.36	15.10	88.59	78.12
4	Ring	Single Row	31	77.01	14.13	81.98	72.04
5	Ring	Single Row	32	78.94	13.30	83.55	74.33
6	Ring	Single Row	32	85.30	15.15	90.55	80.06
7	Ring	Single Row	32	77.70	6.24	79.86	75.54
8	Ring	Single Row	32	74.75	9.62	78.08	71.41
9	Ring	Single Row	30	72.27	12.16	76.62	67.92

Table A.13: Impact angle Analysis : Ring finger single row conditions, mean, standard deviation and 95% confidence interval.

Target	Finger	Condition	N Rows	Mean	Std Dev.	Upper 95% CI	Lower 95% CI
1	Index	Lower	32	78.80	12.53	83.14	74.46
2	Index	Lower	32	74.38	12.08	78.57	70.20
3	Index	Lower	32	67.46	15.75	72.92	62.01
4	Index	Lower	32	52.91	12.91	57.38	48.44
5	Index	Lower	32	53.67	11.08	57.51	49.84
6	Index	Lower	31	51.70	11.92	55.89	47.50
7	Index	Lower	32	36.77	8.24	39.63	33.91
8	Index	Lower	31	37.53	8.42	40.50	34.57
9	Index	Lower	32	39.71	9.35	42.94	36.47
1	Index	Upper	32	82.12	16.58	87.86	76.37
2	Index	Upper	32	76.83	14.28	81.78	71.88
3	Index	Upper	31	69.15	17.04	75.15	63.16
4	Index	Upper	32	53.61	14.72	58.71	48.51
5	Index	Upper	32	56.06	14.36	61.03	51.08
6	Index	Upper	32	53.72	13.90	58.53	48.90
7	Index	Upper	30	37.13	4.97	38.91	35.35
8	Index	Upper	32	36.54	7.18	39.02	34.05
9	Index	Upper	31	34.03	9.78	37.48	30.59

Table A.14: Impact angle Analysis : Index finger double row conditions, mean, standard deviation and 95% confidence interval.

Target	Finger	Condition	N Rows	Mean	Std Dev.	Upper 95% CI	Lower 95% CI
1	Middle	Lower	31	94.54	18.05	100.90	88.19
2	Middle	Lower	32	88.11	15.10	93.35	82.88
3	Middle	Lower	31	83.28	13.84	88.15	78.41
4	Middle	Lower	31	69.51	9.15	72.73	66.29
5	Middle	Lower	32	68.28	10.98	72.09	64.48
6	Middle	Lower	31	68.19	11.79	72.34	64.04
7	Middle	Lower	32	56.90	13.99	61.75	52.05
8	Middle	Lower	32	55.10	12.78	59.53	50.67
9	Middle	Lower	32	57.34	12.67	61.73	52.95
1	Middle	Upper	32	93.12	19.37	99.83	86.41
2	Middle	Upper	32	84.67	17.56	90.75	78.58
3	Middle	Upper	32	83.77	14.84	88.91	78.62
4	Middle	Upper	31	65.74	10.14	69.30	62.17
5	Middle	Upper	30	65.31	13.55	70.16	60.46
6	Middle	Upper	31	67.87	12.98	72.44	63.30
7	Middle	Upper	31	51.46	9.27	54.73	48.20
8	Middle	Upper	32	52.43	9.28	55.64	49.21
9	Middle	Upper	32	52.04	9.28	55.26	48.82

Table A.15: Impact angle Analysis : Middle finger double row conditions, mean, standard deviation and 95% confidence interval.

Finger	Target																Least Sq Mean
Index	1	A	B	C													89.811895
Index	2					E	F	G	H	I							73.560580
Index	3								H	I	J	K					65.515518
Index	4												L	M			54.062537
Index	5													M	N		52.588634
Index	6													M	N		50.163309
Index	7														N	O	43.141564
Index	8															O	37.574202
Index	9															O	38.494219
Middle	1	A	B														94.679789
Middle	2				D	E	F										78.105223
Middle	3					E	F	G	H								74.245432
Middle	4									I	J	K	L				63.327425
Middle	5							G	H	I	J						66.601822
Middle	6								H	I	J	K					65.232534
Middle	7										J	K	L	M			58.584545
Middle	8										J	K	L	M			57.912454
Middle	9											K	L	M			55.287881
Ring	1	A															99.287479
Ring	2		B	C	D												87.257169
Ring	3			C	D	E											83.356412
Ring	4				D	E	F	G									76.900821
Ring	5				D	E	F										78.941499
Ring	6		B	C	D												85.303740
Ring	7				D	E	F										77.697951
Ring	8					E	F	G	H								74.746304
Ring	9						F	G	H	I							72.744801

Table A.16: Impact Angle Analysis : Post-Hoc test for the impact angle, for the 3 fingers and single row condition

Finger	Condition	Target																	Least Sq Mean
Index	Lower	1			F	G	H	I	J	K	L	M							78.79685
Index	Lower	2					H	I	J	K	L	M	N						74.38145
Index	Lower	3										M	N	O	P				67.46269
Index	Lower	4															R		52.90841
Index	Lower	5															R		53.67454
Index	Lower	6															R		51.95176
Index	Lower	7																S	36.76998
Index	Lower	8																S	37.50163
Index	Lower	9																S	39.70532
Index	Upper	1	D	E	F	G	H	I	J										82.11707
Index	Upper	2				G	H	I	J	K	L	M	N						76.83394
Index	Upper	3										M	N						69.01988
Index	Upper	4															R		53.61112
Index	Upper	5													P	Q	R		56.05689
Index	Upper	6															R		53.71832
Index	Upper	7																S	37.25658
Index	Upper	8																S	36.53795
Index	Upper	9																S	33.94452

Table A.17: Impact Angle Analysis : Post-Hoc test for the impact angle, for the index finger and double rows condition

Finger	Condition	Target																		Least Sq Mean
Middle	Lower	1	A	B	C															94.51179
Middle	Lower	2		B	C	D	E	F	G											88.11483
Middle	Lower	3			C	D	E	F	G	H	I	J								83.53726
Middle	Lower	4											L	M	N					69.47491
Middle	Lower	5												M	N	O				68.28447
Middle	Lower	6												M	N	O				68.44092
Middle	Lower	7														O	P	Q	R	56.90046
Middle	Lower	8																Q	R	55.09924
Middle	Lower	9														O	P	Q	R	57.33721
Middle	Upper	1	A	B	C	D														93.12073
Middle	Upper	2			C	D	E	F	G	H	I									84.66705
Middle	Upper	3			C	D	E	F	G	H	I									83.76531
Middle	Upper	4													N	O	P	Q		65.98984
Middle	Upper	5													N	O	P	Q		65.83623
Middle	Upper	6												M	N	O				67.84078
Middle	Upper	7																	R	51.43265
Middle	Upper	8																	R	52.42734
Middle	Upper	9																	R	52.04019

Table A.18: Impact Angle Analysis : Post-Hoc test for the impact angle, for the middle finger and double rows condition

Finger	Condition	Target															Least Sq Mean
Ring	Lower	1	A														101.29696
Ring	Lower	2		B	C	D	E	F									88.96059
Ring	Lower	3	A	B	C	D	E										90.93813
Ring	Lower	4				D	E	F	G	H	I	J	K				81.94420
Ring	Lower	5		B	C	D	E	F	G								87.61909
Ring	Lower	6	A	B	C	D	E	F									89.83836
Ring	Lower	7				D	E	F	G	H	I	J					82.60161
Ring	Lower	8			C	D	E	F	G	H							84.95699
Ring	Lower	9		B	C	D	E	F	G								86.34669
Ring	Upper	1	A	B													97.03621
Ring	Upper	2	A	B	C	D	E										90.36557
Ring	Upper	3	A	B	C	D	E	F									89.74847
Ring	Upper	4					E	F	G	H	I	J	K	L			81.08587
Ring	Upper	5						F	G	H	I	J	K	L	M		78.68886
Ring	Upper	6					E	F	G	H	I	J	K				81.45117
Ring	Upper	7									I	J	K	L	M	N	73.24189
Ring	Upper	8										J	K	L	M	N	71.92642
Ring	Upper	9											K	L	M	N	70.35754

Table A.19: Impact Angle Analysis : Post-Hoc test for the impact angle, for the ring fingers and double rows condition

Bibliography

3GearSystemsInc. 3gear systems, 2013. URL `https://threegear.com/`.

A Agnihotri, B Purwar, N Jeebun, and S Agnihotri. Determination of sex by hand dimensions. *Internet Scientific Publication of Forensic Science*, 2005. URL `http://ispub.com/IJFS/1/2/9047#`.

Salvador Cobos, Manuel Ferre, Sanchez Uran, Javier Ortego, and Cesar Pena. Efficient human hand kinematics for manipulation tasks. In *Intelligent Robots and Systems, 2008. IROS 2008. IEEE/RSJ International Conference on*, pages 2246–2251. IEEE, 2008.

Niloofar Dezfuli, Mohammadreza Khalilbeigi, Jochen Huber, Florian Müller, and Max Mühlhäuser. Palmrc: imaginary palm-based remote control for eyes-free television interaction. In *Proceedings of the 10th European conference on Interactive tv and video*, pages 27–34. ACM, 2012.

Leah Findlater, Jacob O Wobbrock, and Daniel Wigdor. Typing on flat glass: examining ten-finger expert typing patterns on touch surfaces. In *Proceedings of the SIGCHI conference on Human factors in computing systems*, pages 2453–2462. ACM, 2011.

L Gillam, R McDonald, FJP Ebling, and TM Mayhew. Human 2d (index) and 4d (ring) finger lengths and ratios: cross-sectional data on linear growth patterns, sexual dimorphism and lateral asymmetry from 4 to 60 years of age. *Journal of anatomy*, 213(3):325–335, 2008.

Sean Gustafson, Daniel Bierwirth, and Patrick Baudisch. Imaginary interfaces: spatial interaction with empty hands and without visual feedback. In *Proceedings of the 23nd annual ACM symposium on User interface software and technology*, pages 3–12. ACM, 2010.

Sean Gustafson, Christian Holz, and Patrick Baudisch. Imaginary phone: learning imaginary interfaces by transferring spatial memory from a familiar device. In *Proceedings of the 24th annual ACM symposium on User interface software and technology*, pages 283–292. ACM, 2011.

Sean G Gustafson, Bernhard Rabe, and Patrick M Baudisch. Understanding palm-based imaginary interfaces: the role of visual and tactile cues when browsing. In *Proceedings of the SIGCHI Conference on Human Factors in Computing Systems*, pages 889–898. ACM, 2013.

Elise Hancock. A primer on touch, 1996. URL `http://pages.jh.edu/~jhumag/996web/touch.html`.

Chris Harrison, Shilpa Ramamurthy, and Scott E Hudson. On-body interaction: armed and dangerous. In *Proceedings of the Sixth International Conference on Tangible, Embedded and Embodied Interaction*, pages 69–76. ACM, 2012.

Franchesca V. Havas. Your glove size. URL `http://www.purplemath.com/modules/boxwhisk.htm`.

Healthline. Body maps : Flexor digiti minimi brevis (hand), 2005. URL `http://www.glove.org/Modern/glovemeasure.php`.

Christian Holz and Patrick Baudisch. The generalized perceived input point model and how to double touch accuracy by extracting fingerprints. In *Proceedings of the SIGCHI Conference on Human Factors in Computing Systems*, pages 581–590. ACM, 2010.

Andreas Kolb, Erhardt Barth, Reinhard Koch, and Rasmus Larsen. Time-of-flight sensors in computer graphics. In *Proc. Eurographics (State-of-the-Art Report)*, pages 119–134, 2009.

Lynn S Lippert. *Clinical kinesiology and anatomy*. FA Davis, 2011.

Roman Lissermann, Jochen Huber, Aristotelis Hadjakos, and Max Mühlhäuser. Earput: augmenting behind-the-ear devices for ear-based interaction. In *CHI'13 Extended Abstracts on Human Factors in Computing Systems*, pages 1323–1328. ACM, 2013.

Jiake Liu. Gauntlet : The glove keyboard, January 2012. URL `http://gauntletkeyboard.com/`.

Christian Loclair, Sean Gustafson, and Patrick Baudisch. Pinchwatch: a wearable device for one-handed microinteractions. In *Proc. MobileHCI*, 2010.

Carsten Mehring, Falko Kuester, Kunal Deep Singh, and Michelle Chen. Kitty: Keyboard independent touch typing in vr. In *VR*, pages 243–244, 2004.

Pranav Mistry and Pattie Maes. Sixthsense: a wearable gestural interface. In *ACM SIGGRAPH ASIA 2009 Sketches*, page 11. ACM, 2009.

Santosh Rath. Hand kinematics: Application in clinical practice. indian j plast surg 2011;44:178-85, 2011. URL `http://www.ijps.org/text.asp?2011/44/2/178/85338`.

RHLVisionTechnologies. Fin : Wearable ring, January 2014. URL `http://www.wearfin.com/`.

Elizabeth Stapel. Box-and-whisker plots: Interquartile ranges and outliers, July 2014. URL `http://www.healthline.com/human-body-maps/flexor-digiti-minimi-brevis-hand`.

ThalmicLabs. Myo, June 2013. URL `http://gauntletkeyboard.com/`.

Daniel Vogel and Patrick Baudisch. Shift: a technique for operating pen-based interfaces using touch. In *Proceedings of the SIGCHI conference on Human factors in computing systems*, pages 657–666. ACM, 2007.

Feng Wang and Xiangshi Ren. Empirical evaluation for finger input properties in multi-touch interaction. In *Proceedings of the SIGCHI Conference on Human Factors in Computing Systems*, pages 1063–1072. ACM, 2009.

Wikipedia. Proprioception — Wikipedia, the free encyclopedia, 2003. URL `http://en.wikipedia.org/wiki/Proprioception`.

Zhengyou Zhang. Microsoft kinect sensor and its effect. *MultiMedia, IEEE*, 19(2):4–10, Feb 2012. ISSN 1070-986X. doi: 10.1109/MMUL.2012.24.

Index

Typeset August 4, 2014